Original Article

Histological Study of the Effect of Pristine Versus Functionalized Polyethylene Glycol - Multiwalled Carbon Nanotubes on the Lung Alveoli of the Adult Male Albino Rats

Safinaz Hussein Safwat, Iman Nabil, Wahid Stephanos and Marwa Magdi

Histology and Cell Biology Department, Faculty of Medicine, University of Alexandria, Egypt

ABSTRACT

Background: Carbon nanotubes are used in a variety of applications. However, their toxicity on different body tissues has an impact on human health. Therefore, functionalization emerged as a tool to reduce CNTs toxicity and hence expand their applications.

Aim: The goal of this study was to clarify the impact of pristine MW CNTs on lung alveoli of the adult male albino rat and the possibility of amelioration of this effect by functionalized PEG-MWCNTs.

Materials and Methods:60 adult male rats were categorized among 3 groups. Group I: control group, group II: 20 rats received an intratracheal instillation of a single dose of 1 mg/kg of pristine MWCNTs, then subdivided into two equal subgroups (each 10 rats) and were sacrificed after 3 days and 45 days respectively, group III: 20 rats were received an intratracheal instillation of a single dose of 1 mg/kg of PEG-MWCNTs and then subdivided and sacrificed as in group II. At the end of the experiment, the lungs were harvested for histological examination. The thickness of the interalveolar septum and the collagen area were morphometrically evaluated and statistically analyzed.

Results: Pristine MWCNTs caused variable degree of histological changes that were more evident after 45 days. These changes manifested by collapsed alveoli alternating with wide ones, thickening of the interalveolar septa, deposition of collagen, cellular and nuclear changes suggestive of pulmonary toxicity and accumulation of particulate laden macrophages. Morphometric and statistical studies demonstrated significant increase in the thickness of the interalveolar septa as compared to control group. Ultrastructurally, type II pneumocytes showed degenerative changes and formed the predominant cell lining. The changes were less evident by instillation of functionalized PEG-MWCNTs with more or less preservation of the normal alveolar architecture.

Conclusion: Pristine MWCNTs have a toxic effect on the lung tissue which could be reduced by functionalized PEG-MWCNTs.

Received: 15 May 2019, **Accepted:** 13 June 2019

Key Words: Carbon nanotubes, histology, polyethylene glycol, pristine.

Corresponding Author: Iman Nabil, MD, Histology and Cell Biology Department, Faculty of Medicine, University of Alexandria, Egypt, **Tel.**: +20 1004149637, **E-mail:** emannabil4@gmail.com

ISSN: 1110-0559, Vol. 42, No. 4

INTRODUCTION

Nanotechnology is defined as the knowledge and control of materials at dimensions engineered in nanoscale, where unique phenomena enable novel applications. Nanoparticles (NPs) are processed from nanomaterials and defined as particles whose size can be measured in nanometers[1].

Nowadays, it is well established that NPs have high surface area to volume ratios. This character is a double-edged sword, allowing specific interactions to occur between nanoparticles and several biomolecules of the same range in nanoscale, making NPs highly versatile for different applications, but it is accompanied by the liability of NPs to produce cytotoxicity and put human health in danger[2].

Mainly there are two groups in which the NPs are categorized; organic and inorganic NPs. On account of the ability of the inorganic NPs to tolerate unfavorable processing conditions, they possess nowadays a great importance[3]. Depending on the physical and chemical properties of the nanoparticles, they are classified into: carbon-based-nanostructures, metal oxide NPs, organic polymers, liposomes, quantum dots and dendrimers. The molecular bases of carbon-based nanostructures are pure carbons in which they are classified into two essential groups; fullerenes and carbon nanotubes (CNTs)[4].

Carbon nanotubes are a cylinder like material made up of pure carbon with diameters of nanometer and lengths of many microns. Two types of carbon nanotubes are well categorized, either single-walled carbon nanotubes or multi-walled carbon nanotubes. A single-walled carbon nanotubes (SWNTs) are formed from rolling of a sheet of graphite into seamless cylinder, whereas multi-walled nanotubes (MWNTs) are consisted of several concentric nanotube sheets[5].

 DOI: 10.21608/ejh.2019.12809.1119

Commercially, carbon nanotubes are employed in varieties of applications involved in industry, engineering, medicine and agriculture[6]. CNTs own distinguishing features such as stability, flexibility, stiffness, strength, thermal and electrical conductivity[7]. Furthermore, CNTs have a very unique characteristic feature which is an ultrahigh surface area compared to mass; this ratio depends on two factors: CNTs' diameter and the extent to which they form bundles[8]. By this property, CNTs play an important role in drug delivery inside human cells in which the drug can be integrated to walls of CNTs and bind specific receptors on the cell surface. In the context, the drugs could be loaded on CNTs and enter any body cell by mean of endocytosis, thus giving the most benefit of the therapy with the least side effects to the other cells[9,10].

There are many different routes for administration of CNTs in the body. These ways involve: oral, intravenous injection, inhalation and intraperitoneal administration. Inside the body, CNTs either interact with different biological elements as proteins or cells which finally lead either to retaining their original structure; be metabolized or they can be distributed inside the body to remain or excreted. Unfortunately, the time taken for these processes to occur is not yet known[11]. Respiratory system toxicity takes the priority among any other systems in the body in which CNTs can produce a toxic effect. This is due to the quick absorption and deposition of the tiny-sized CNTs which is dispersed in the air and inhaled in the lungs causing pulmonary toxicity[12].

CNTs' toxicity and reactivity differ according to many factors such as the length and the diameter of the fiber, surface area, tendency to agglomerate, dispersion in media, and the manner used for their manufacture. It should obviously bear in mind that the insolubility of pristine CNT can be fixed by chemical functionalization that also modify the efficacy of CNTs[13].

In order to reduce the cytotoxicity of CNTs and extend their biomedical applications, it is important to improve their solubility and dispersion. The physiochemical properties of CNTs can be modified by functionalization in which the size of the added functional group and the type of chemical modification (whether covalent or non-covalent) can alter its biological toxicity[14].

Covalent functionalization can be processed by attaching molecules to the CNTs' backbone. This method caused change of the tube sidewall which affected the properties of the nanotubes. On the other hand, non-covalent functionalization of CNTs is just adsorption of molecules onto the nanotube surface with resultant preservation of most of their properties[15,16].

For biological applications, the usage of oligoethylene glycol (OEG) or Polyethylene glycol (PEG) is to stabilize the anchored biomolecules and to reduce any other non-preferred materials to adsorb onto CNTs. So far, PEG was used to functionalize CNTs in order to reduce its toxicity[12].

Thus, the present work was designed to investigate the light and electron microscopic changes that might occur in the lung alveoli of adult male albino rats after the intratracheal administration of pristine and the possible amelioration of this effect by functionalized PEG –coated MWCNTs.

MATERIALS AND METHODS

Materials for preparation of multi-walled carbon nanotubes: Pristine MWCNTs and functionalized PEG-coated MWCNTs were purchased from Nano Tech Egypt (6th October, Giza, Egypt) and suspended in sterile 0.9% saline containing 0.1% Tween 80. Immediately before in *vivo* administration, sonication of the suspensions occurred for 15 min with an ultrasonic sonopuls in a short break every two minutes, followed by vortexing the suspension on ice to further force the CNTs dispersion[13].

Characterization of multiwalled carbon nanotubes

A-Transmission electron microscopy (TEM): For measuring the size and visualize the shape of CNTs using a Jeol 100 CX electron microscope (Tokyo, Japan). After preparation of pristine MWCNTs and functionalized PEG-coated MWCNT solution, a droplet was sited onto a copper grid coated with carbon and left to evaporate[17].

B-Fourier-transform infrared (FTIR) spectra: To recognize the existence of an organic molecule or a functional group using a Shimadzu FTIR-8400S (Tokyo, Japan). Centrifugation of 10 ml of a prepared solution of pristine multi-walled carbon nanotubes and functionalized polyethylene glycol (PEG) coated MWCNT occurred at 4000 rpm for 10 min followed by redispersion in 20 ml of sterile water and centrifuged again. These processes were repeated three times[18]. The spectra were recorded over the wave number range of 350-4400cm−1.

Animals

Sixty adult male albino rats (150-200g) were obtained from the animal house of Institute of Graduate Studies and Research, Alexandria University. The animals were allowed to adapt for 2 weeks before the experiment. The animals were maintained under standard laboratory conditions of temperature and humidity and 12 hours light/dark cycle. All experimental trials were accepted and meeting the requirements with the guide lines of the Local Ethical Committee of the Faculty of Medicine, University of Alexandria.

Experimental design

The rats were randomly divided into three groups as following:

Group I: 20 rats served as a control group, were received intratracheal instillation of a single dose of 1 ml/kg body weight saline once at the beginning of the experiment and was subdivided into two equal subgroups; subgroup IA: 10 rats were sacrificed after 3 days and subgroup IB: 10 rats were sacrificed after 45 days.

Group II: 20 rats serving as an experimental group received intratracheal instillation of a single dose of 1 mg/kg body weight[13] of the pristine MWCNTs once at the beginning of the experiment. The animals were subdivided into two equal subgroups; subgroup IIA: 10 rats were sacrificed after 3 days and subgroup IIB: 10 rats sacrificed after 45 days.

Group III: 20 rats serving as an experimental group received intratracheal instillation of a single dose of 1 mg/kg body weight[13] of functionalized PEG- coated MWCNTs. The animals were subdivided into 2 subgroups; subgroup IIIA: 10 rats were sacrificed after 3 days and subgroup IIIB: 10 rats were sacrificed after 45 days.

Histological study

At the end of each experiment (after 3 days and 45 days), all the rats were sacrificed under anesthesia. The two lungs of each rat were obtained, one of them was processed for light microscopic examination and the other was processed for electron microscopic examination.

1. Light microscopy: Lung specimens were fixed in 10% formol saline, dehydrated in ascending grades of alcohol, cleared in xylol and embedded in paraffin. 5µm thick paraffin sections were obtained and stained by hematoxylin and eosin (HandE) and Tichrome stains[19].
2. Transmission electron microscopy: Lung specimens were obtained, cut into 1 mm^3, fixed in 3% phosphate buffer glutaraldehyde at pH 7.4 for 1 day at 4 °C and then processed to get ultrathin stained sections[20]. Electron micrographs were obtained by using TEM (Jeol 100 CX, Tokyo, Japan) equipped with a digital camera at the electron microscopy unit, Faculty of Science, University of Alexandria.

Morphometric study

Digital images from HandE and Trichrome stained sections were obtained using a digital camera (Olympus DP20) connected to microscope (Olympus BX41). The images from HandE stained sections were used to determine the thickness of the interalveolar septum. On the other hand, Trichrome stained sections were used to determine the percentage area of collagen. Interalveolar septum thickness in (µm) and the percentage area of the collagen (%) were analyzed histomorphometrically using NIH Image j (v1.49) software.

Statistical analysis

Data obtained from the morphometry were fed to the computer and analyzed using IBM SPSS software package version 20.0. (Armonk, NY: IBM Corp). The Kolmogorov-Smirnov, Shapiro and D'agstino tests were used to verify the normality of distribution of variables, ANOVA was used for comparing the five studied groups and followed by Post Hoc test (Tukey) for pairwise comparison. While Kruskal Wallis test was used to compare five groups for abnormally distributed quantitative variables and followed by Post Hoc test (Dunn's for multiple comparisons test) for pairwise comparison. Significance of the obtained results was judged at the 5% level.

Results

Characterization of the MWCNTs

1. Transmission electron microscopy (TEM): The TEM of the pristine and functionalized PEG-coated MWCNTs showed that they were fiber-like of different lengths and diameters. The diameter of pristine-MWCNTs ranges between 5.17-9.46 nm, while that of functionalized PEG-coated MWCNTs ranges between 14.6-16.8 nm. (Figure 1a, b).
2. Fourier transform infrared spectroscopic analysis (FTIR): The FTIR spectra of pristine MWCNTs and the PEG-coated MWCNTs were shown in (Figure 2a and Figure 2b) respectively. The characteristic bands due to generated functional groups were observed in the spectrum of PEG-coated MWCNTs. In (Figure 2a) we could not see any band compared with the functionalized MWCNTs. The PEG-coated MWCNTs showed new peaks in comparison with the FITR spectrum of the pristine MWCNTs (Figure 2a, b).

Histological results

1-Light microscopic results

a-Hematoxylin and eosin stain

Control group (Group I)

Examination of sections of the lung tissue of the control group (subgroup IA and subgroup IB) revealed normal histological structure of the alveolar tissue. The alveoli were patent. They were lined by two types of pneumocytes; flat type I pneumocytes forming the main type of alveolar lining and few type II pneumocytes bulging in the lumen. The alveoli were separated by thin inter-alveolar septa. Blood capillaries were seen inside the interalveolar septa. They appeared with thin wall ramifying in between the alveoli surrounded by few interstitial cells (Figure 3a, b).

Group II (animals received pristine MWCNTs)

Subgroup IIA (sacrificed after 3 days): Examination of sections of the lung of rats of this subgroup revealed evident histological alterations with many areas of collapsed alveoli. The inter-alveolar septa showed an apparent thickening. Areas of perivascular and peribronchiolar cellular infiltration were observed. Congested blood vessels were also encountered (Figure 4). Cytoplasmic vacuolations were seen in the epithelial lining of the alveoli. Black particles were noticed in the interalveolar septa (Figure 5)

Subgroup IIB (sacrificed after 45 days): Examination of sections of the lung of rats of this subgroup showed an apparent thickening of the interalveolar septa. Cellular

infiltration and hyalinization were observed inside the interalveolar septa. Most of alveoli were collapsed, while other appeared wide. Black particles of CNTs and marked extravasated RBCs were observed in the interalveolar septa and in the alveolar cavities (Figures 6-8)

Group III (animals received functionalized PEG-coated MWCNTs)

Subgroup IIIA (sacrificed after 3 days): Many lung alveoli of the rats of this subgroup were quite well aerated. Apparently thickened interalveolar septa were observed in some areas (Figure 9 a and b)

Subgroup IIIB (sacrificed after 45 days): Examination of this subgroup showed considerable degree of preservation of the alveolar architecture. Most of alveoli were patent and lined with type I pneumocytes and type II pneumocytes. The interalveolar septa were apparently thin. Some areas revealed an apparent thickening of the septa with congested blood vessels and extravasated RBCs (Figure 10a, b)

b-Masson trichrome stain

Examination of Masson trichrome stained sections revealed apparent increase in collagen deposition in pristine –treated rats (group II) as compared to the control group especially in subgroup IIB which sacrificed after 45 days. (Figure 11a-c) On the other hand, the rats received functionalized PEG-coated MWCNTs (group III) showed collagen deposition approximated the control group (Figure 11d,e). These data were further analyzed morphometrically.

Electron microscopic results

Control group (Group I)

Electron microscopic examination of ultrathin sections of the lung of two control subgroups IA and IB revealed normal histological appearance with well inflated alveoli lined by type I and type II pneumocytes. Type I were the predominant one with elongated euchromatic nuclei. Type II pneumocytes showed euchromatic nuclei, characteristic microvillous border and multiple lamellar bodies. The interalveolar septa appeared thin and revealed many blood capillaries and few interstitial cells (Figures 12,13)

Group II [animals received pristine MWCNTs]

Subgroup IIA (sacrificed after 3 days): Examination of ultrathin sections of the rat lung of this group revealed obvious histological alteration of alveolar architecture with wide areas of collapsed alveoli. The alveoli were lined mainly with type II pneumocytes. They revealed irregular nuclei and empty lamellar bodies (Figure 14). Some cells of type I pneumocytes revealed irregular nuclei and were seen bulging into the alveolar lumen. The interalveolar septa were somewhat thickened containing many interstitial cells. Most of the examained sections revealed an apparent increase in collagen fibers (Figure 15). The cytoplasm of the alveolar macrophage showed particles of carbon nanotubes either in the lysosomes and mitochondria or free in the cytoplasm (Figure 16a, b). Many inflammatory cells as eosinophils and neutrophils were also noticed (Figure 17a, b).

Subgroup IIB (sacrificed after 45 days): Examination of ultrathin sections of the lung rats of this subgroup showed multiple pneumocytes type II with blunted microvillous border and dilated perinuclear cisternae. Their cytoplasm revealed dilated rough endoplasmic reticulum and multiple empty lamellar bodies. (Figures 18,19) Excess collagen fibers deposition was evident in this subgroup (Figure 20). Considerable number of active alveolar macrophages with numerous lysosomes in their cytoplasm were also seen. Aggregates of electron dense nanoparticles were depicted either free in the cytoplasm or inside their lysosomes. (Figure 21).

Group III (animals received functionalized PEG-coated MWCNTs)

Ultrastructure Examination of lung rat of this group showed significant preservation of the alveolar tissue. They showed patent alveoli lined mainly with pneumocytes type I and type II that retain their normal appearance. The interalveolar septa were thin and exhibited some interstitial cells(Figures 22,24a, b). In subgroup IIIA, few alveoli revealed proliferation of pneumocytes type II (Figure 23).

Morphometric results and statistical analysis

a. Masson trichrome stain and area of collagen: Data in table 1 and figure 25a revealed that the percentage area of collagen in Masson trichrome stained sections was higher in subgroup IIB as compared to the control group. On the other hand, subgroups IIA and IIIA showed moderate increase in collagen deposition than the control group. Comparatively, subgroup IIIB revealed slight increase in deposition of collagen than control group. Although, in all groups the results were statistically insignificant ($p = 0.088$).

b. The thickness of the interalveolar septa: Data in table 2 and figure 25 b revealed that the thickness of the interalveolar septa was significantly increased in subgroups IIA, IIB and IIIA as compared to the control group ($p < 0.001$) which was more evident in subgroup IIB. On the other hand, the thickness of the interalveolar septa in subgroup IIIB was statistically insignificant as compared to the control group, so far, it was statistically significant from other treated subgroups ($p < 0.001$).

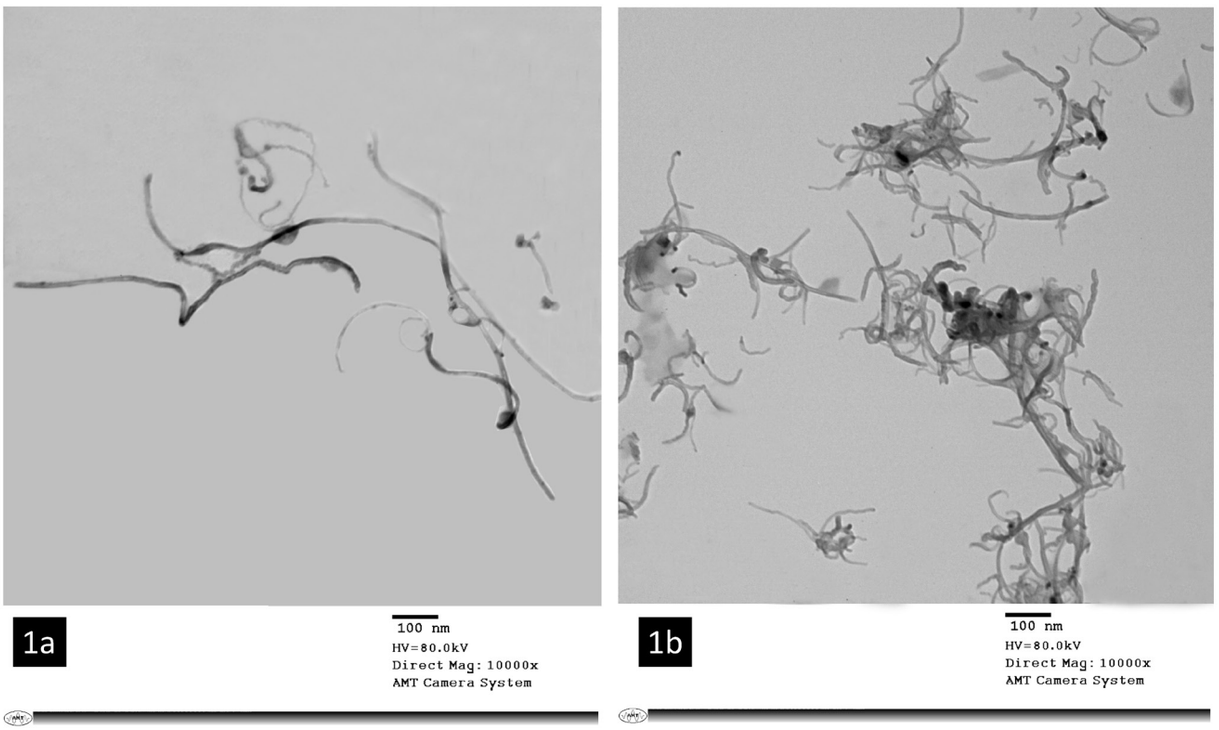

Fig. (1a, b): a-TE micrograph of pristine MWCNTs with an average diameter of 5.17-9.46 nm. b-TE micrograph of functionalized PEG-coated MWCNTs with an average diameter of 14.6-16.8 nm. Mic. Mag. a, b X10000.

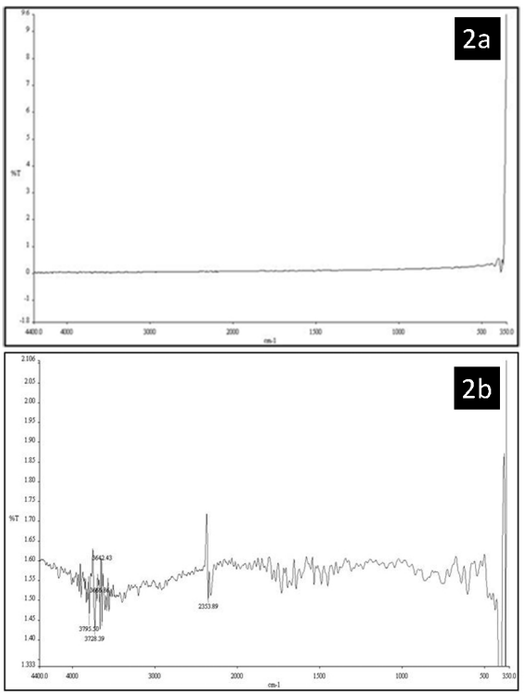

Fig. (2a, b): a-FTIR analysis of pristine MWCNTs does not show any band. b-FTIR analysis of functionalized PEG- coated MWCNTs shows new peak measured at different wave lengths(2353.89, 3642.43,3728.39 and 3795.50cm $^{-1}$).

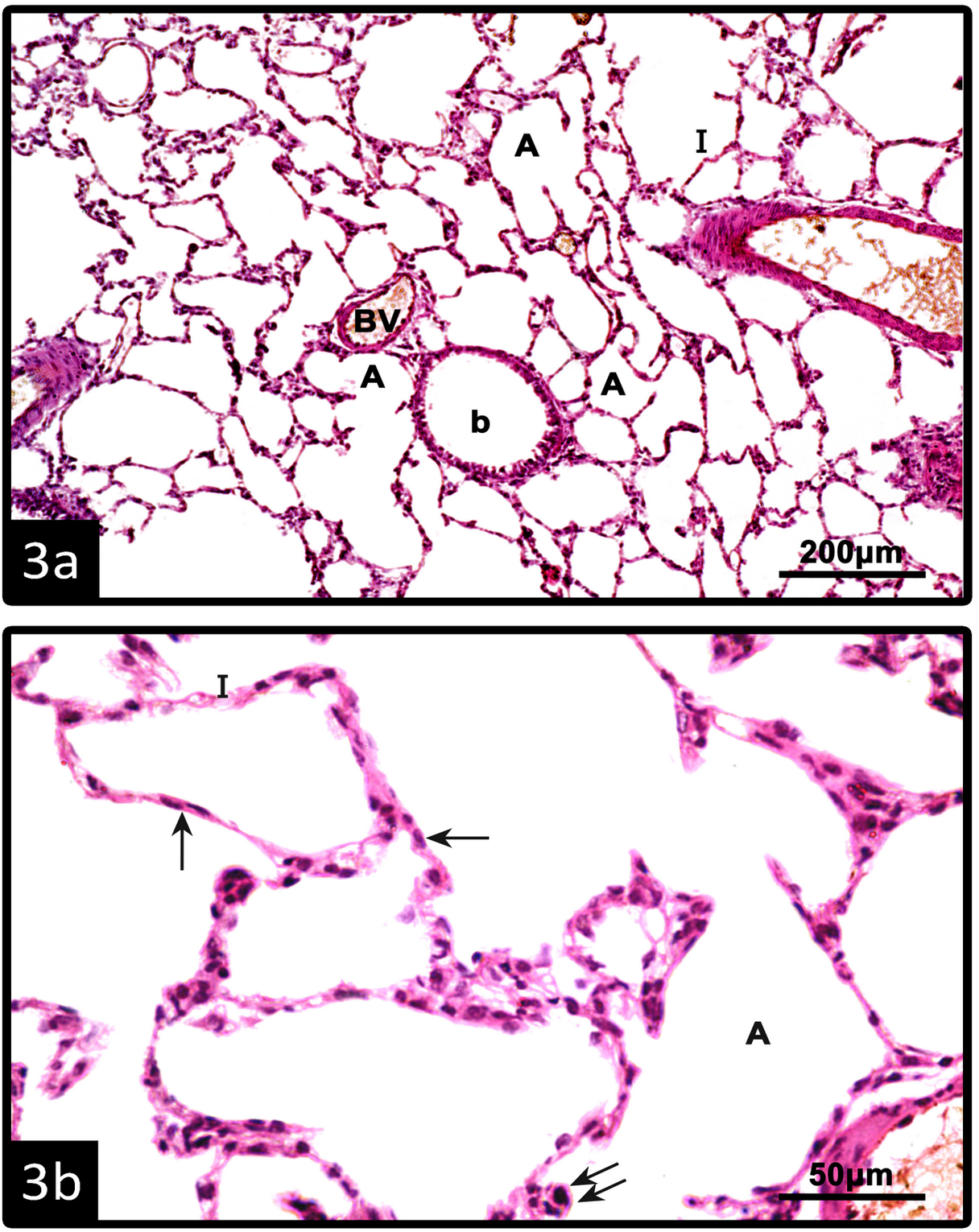

Fig. (3a, b): Photomicrographs of sections of control rat lung showing a-patent alveoli (A) and thin interalveolar septum(I). Blood vessels (BV) and bronchiole (b) are seen. Mic.Mag.x100 b-High power view showing patent alveoli(A) lined by pneumocytes type I(arrow) and pneumocytes type II (double arrows). Thin interalveolar septa(I) with some interstitial cells are seen between the alveoli. Mic.Mag.x400

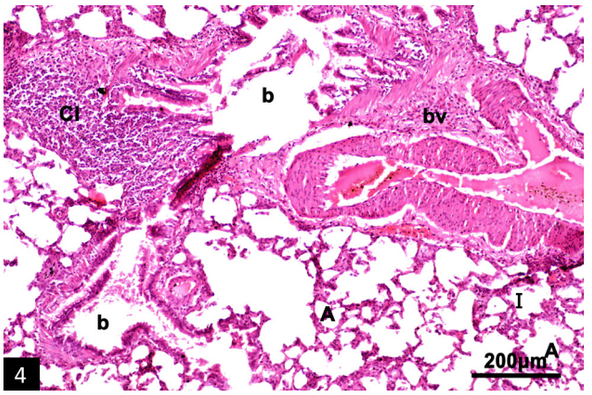

Fig. (4): Photomicrograph of a section of rat lung of subgroup II A (received pristine carbon nanotubes and sacrificed after 3 days) revealing areas of apparently thickened interalveolar septa with some collapsed alveoli(A) while other alveoli appear patent. Marked perivascular and peribronchiolar cellular infiltration(CI) are seen. Note: BV; congested blood vessel with thickened muscular wall. b; bronchiole. Mic.Mag.x100

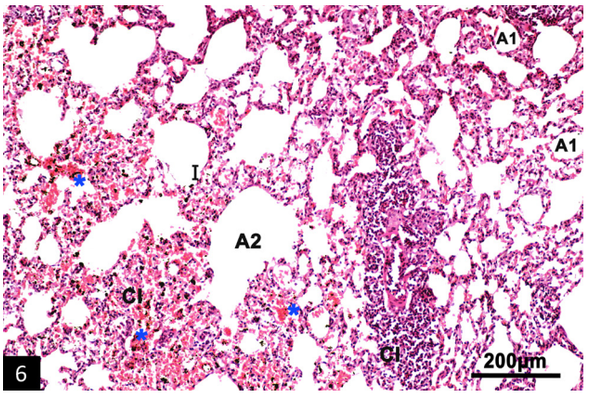

Fig. (6): Photomicrograph of a section of rat lung of subgroup IIB (received pristine carbon nanotubes and sacrificed after 45 days) showing an apparently thick interalveolar septum(I)with marked cellular infiltration(CI). Some of alveoli are collapsed(A1),while others are dilated(A2). Note: extravasated red blood corpuscles (*). Mic.Mag.x100

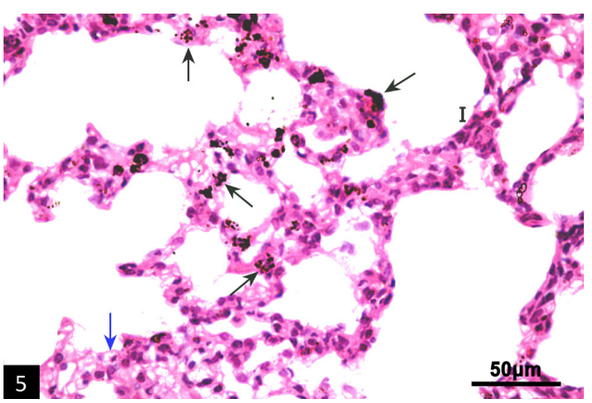

Fig. (5): High power view of a section of rat lung of the same subgroup IIA showing an apparently thickened interalveolar septum(I). Cytoplasmic vacuolations appear in the epithelial lining of the alveoli (blue arrow). Black particles (black arrow) are noticed in the interalveolar septum. Mic.Mag.x400

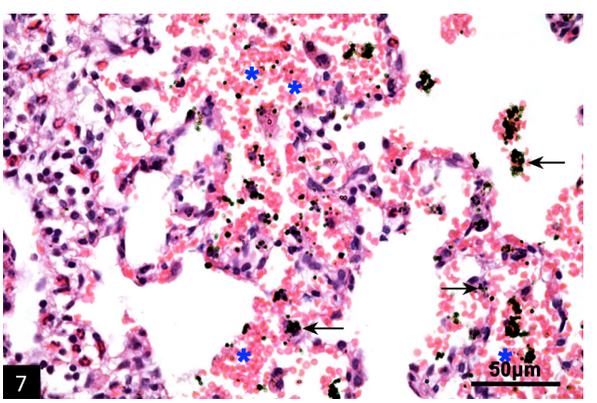

Fig. (7): High magnification of a section of rat lung of subgroup IIB showing an apparent thickening of interalveolar septa. Black particles are encountered in the interalveolar septa and inside the alveolar cavity(arrow). Marked extravasation of red blood corpuscles is also noticed (*). Mic.Mag.x400

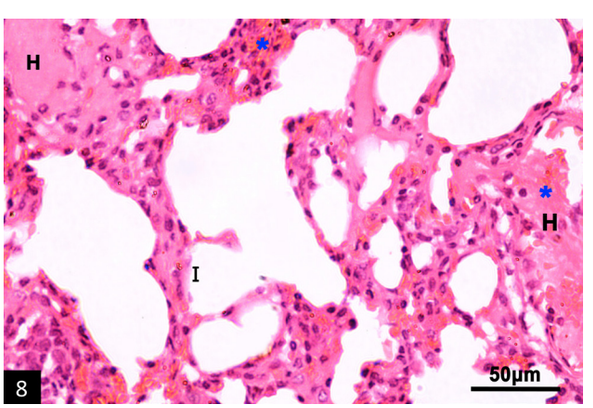

Fig.(8): Photomicrograph of a section of rat lung of the same subgroup IIB showing an apparently thickened interalveolar septum (I) with areas of hyalinization(H)and extravasation of red blood corpuscles (*). Mic.Mag.x400

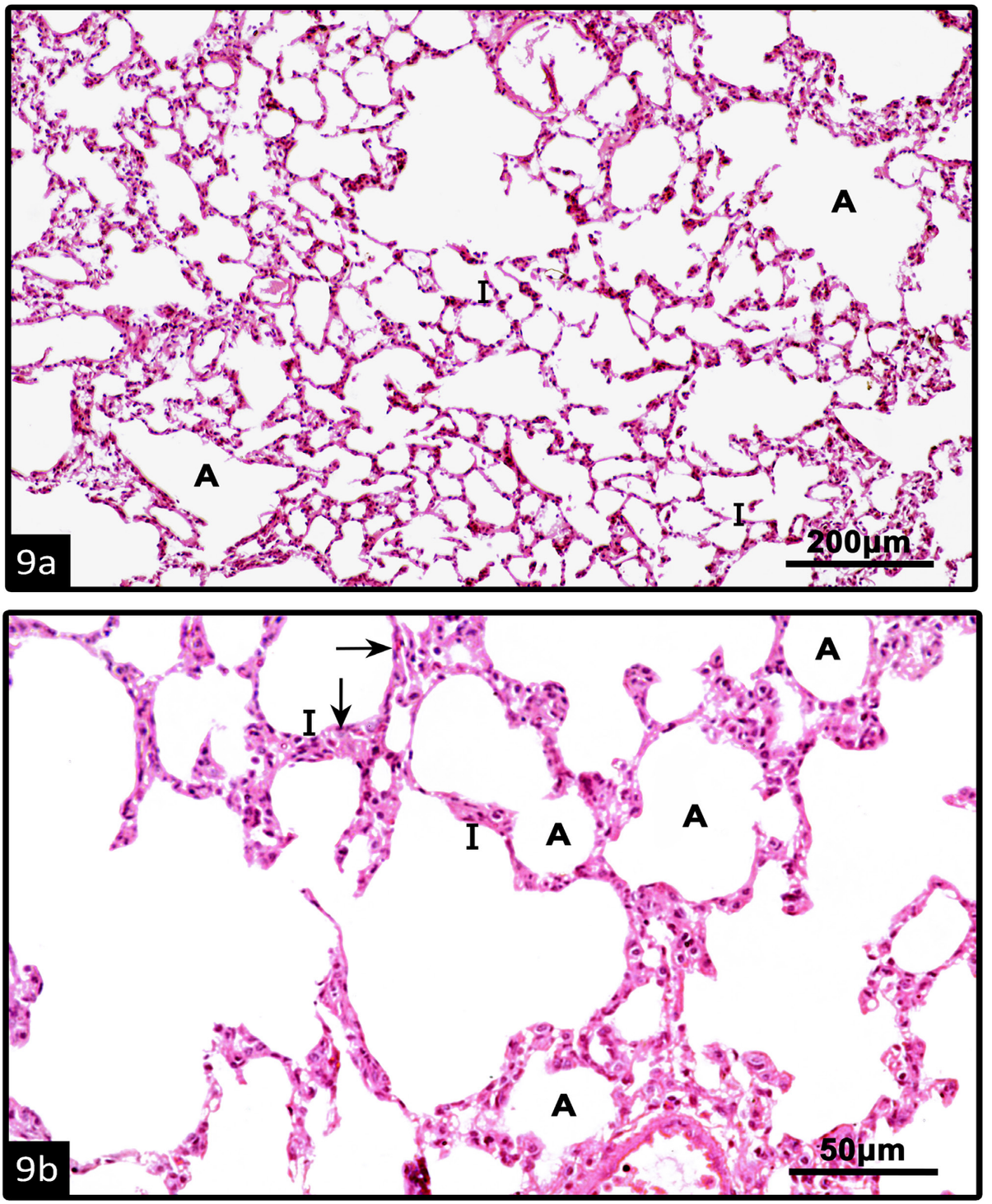

Fig. (9a, b): Photomicrographs of sections of rat lung of the subgroup IIIA (received PEG-coated carbon nanotubes and sacrificed after 3 days) showing a-areas of patent alveoli(A) and an apparent thin interalveolar septum (I). Mic. Mag. x 100 b-In some areas, the septa show an apparent thickening(arrow). Mic. Mag. x400

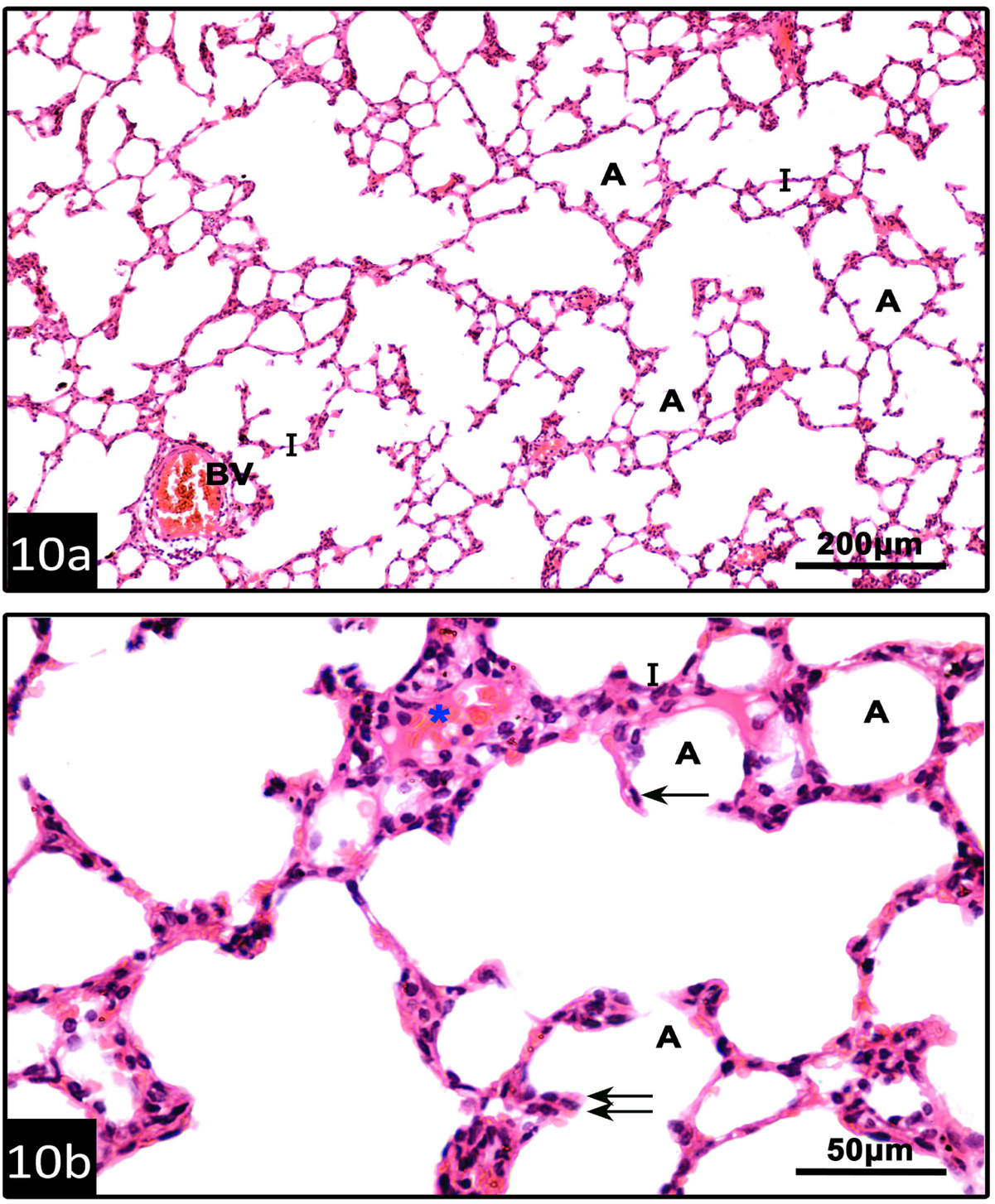

Fig.(10a, b): Photomicrographs of sections of rat lung of the subgroup IIIB (received PEG-coated carbon nanotubes and sacrificed after 45 days) showing a- Areas of patent alveoli(A) with an apparent thin interalveolar septum(I).A congested blood vessel is seen(BV).Mic.Mag.x100 b-High power view showing areas of patent alveoli(A)lined by type I pneumocytes(arrow) and typeII pneumocytes(double arrow). The interalveolar septa (I) reveal an apparent thickening in some areas. Note: extravasated RBCs (*). Mic.Mag.x400

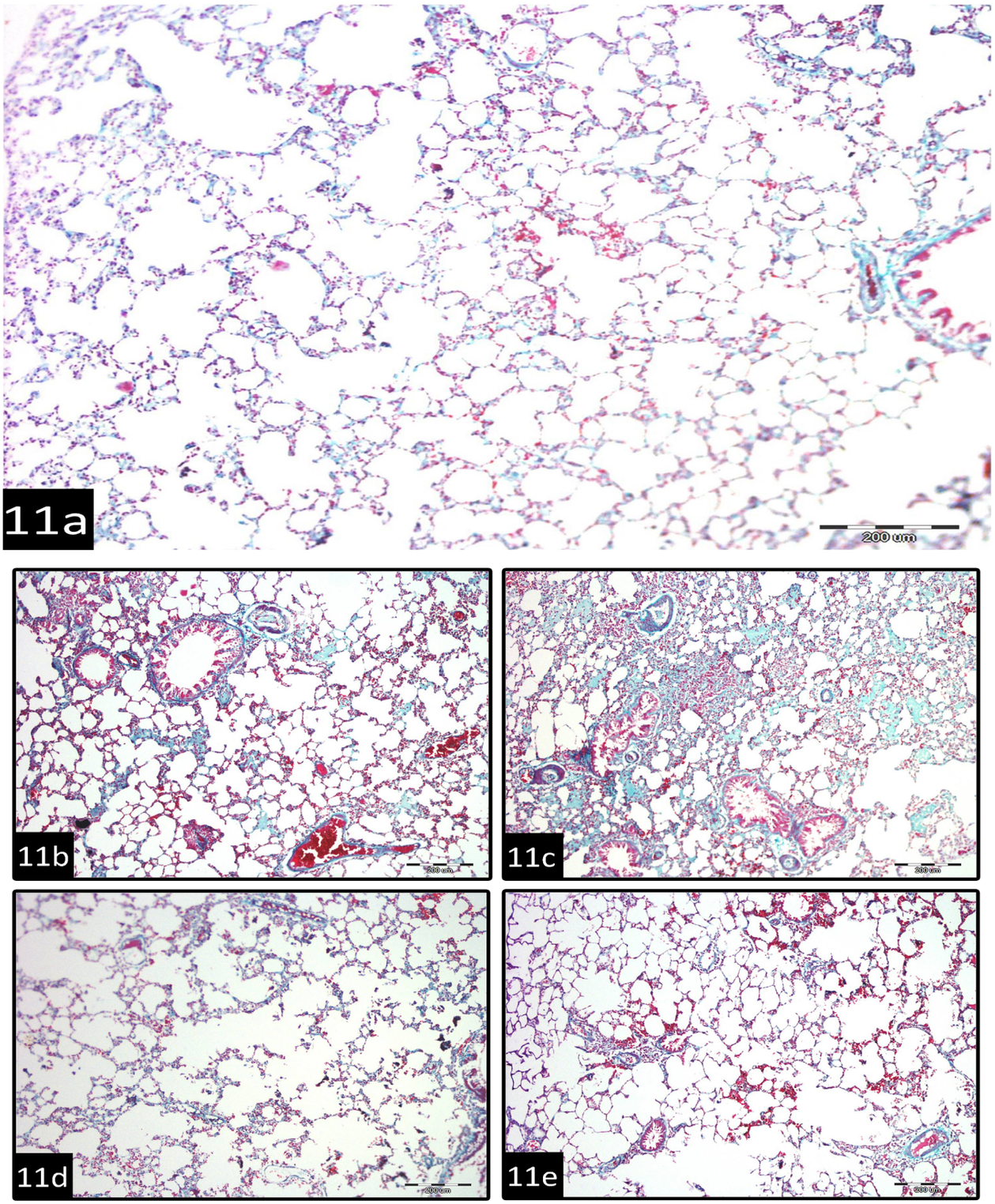

Fig. (11 a-e): Photomicrographs of sections of rat lungs of the different groups stained by Masson trichrome showing different degree of collagen deposition in the interalveolar septa. a-control group showing normal collagen deposition. b-subgroup IIA revealed moderate increase in collagen deposition. c- subgroup IIB illustrating marked increase in deposition of collagen. d-subgroup IIIA with mild collagen deposition. e-subgroup IIIB: collagen deposition is more or less similar to control group. Mic. Mag a-e x 100

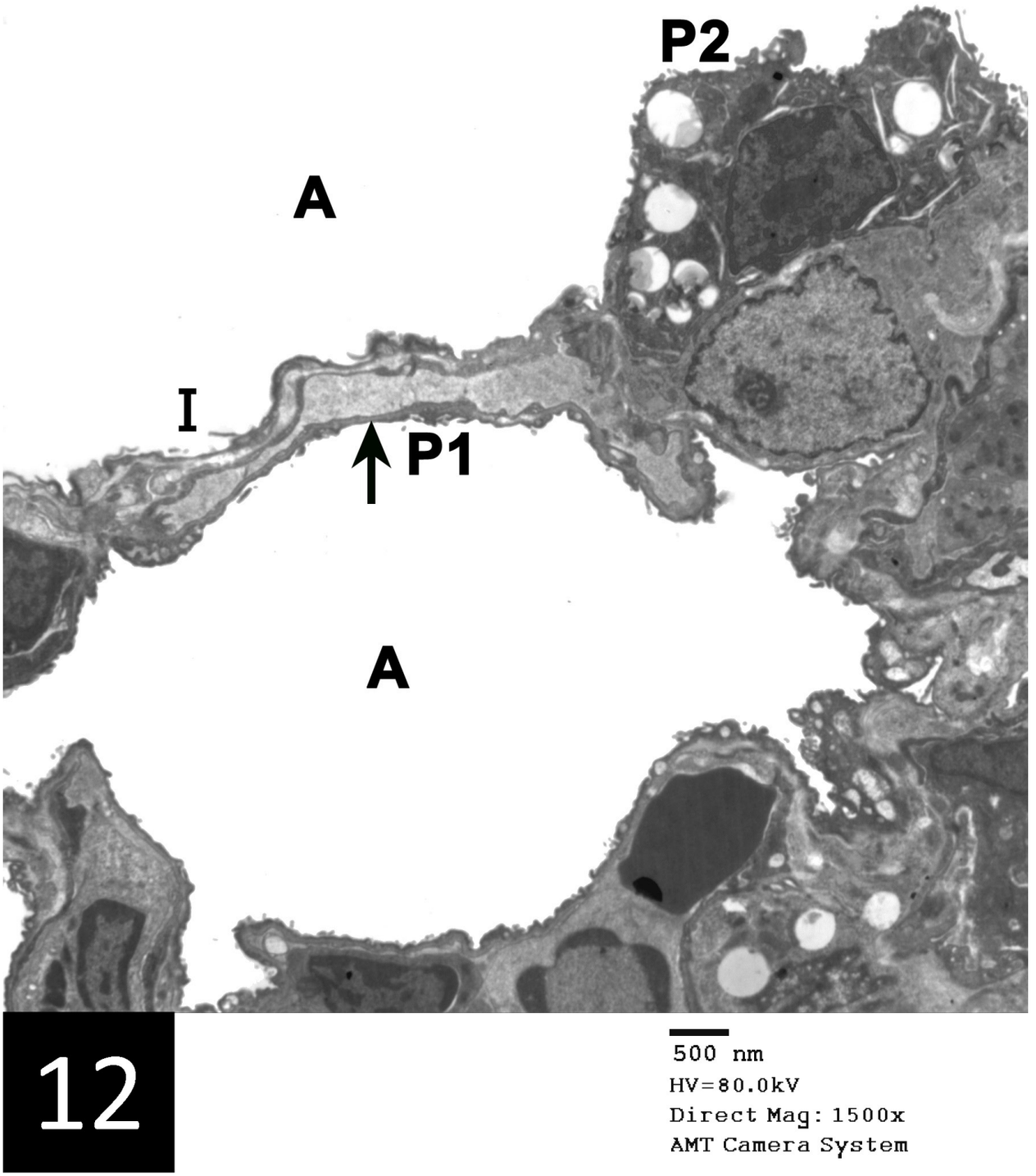

Fig. (12): An electron micrograph of control rat lung showing patent alveoli(A)and thin interalveolar septum(I). Pneumocyte type I (P1) and pneumocyte type II(P2) are seen lining the alveolar lumen. Mic. Mag. x1500

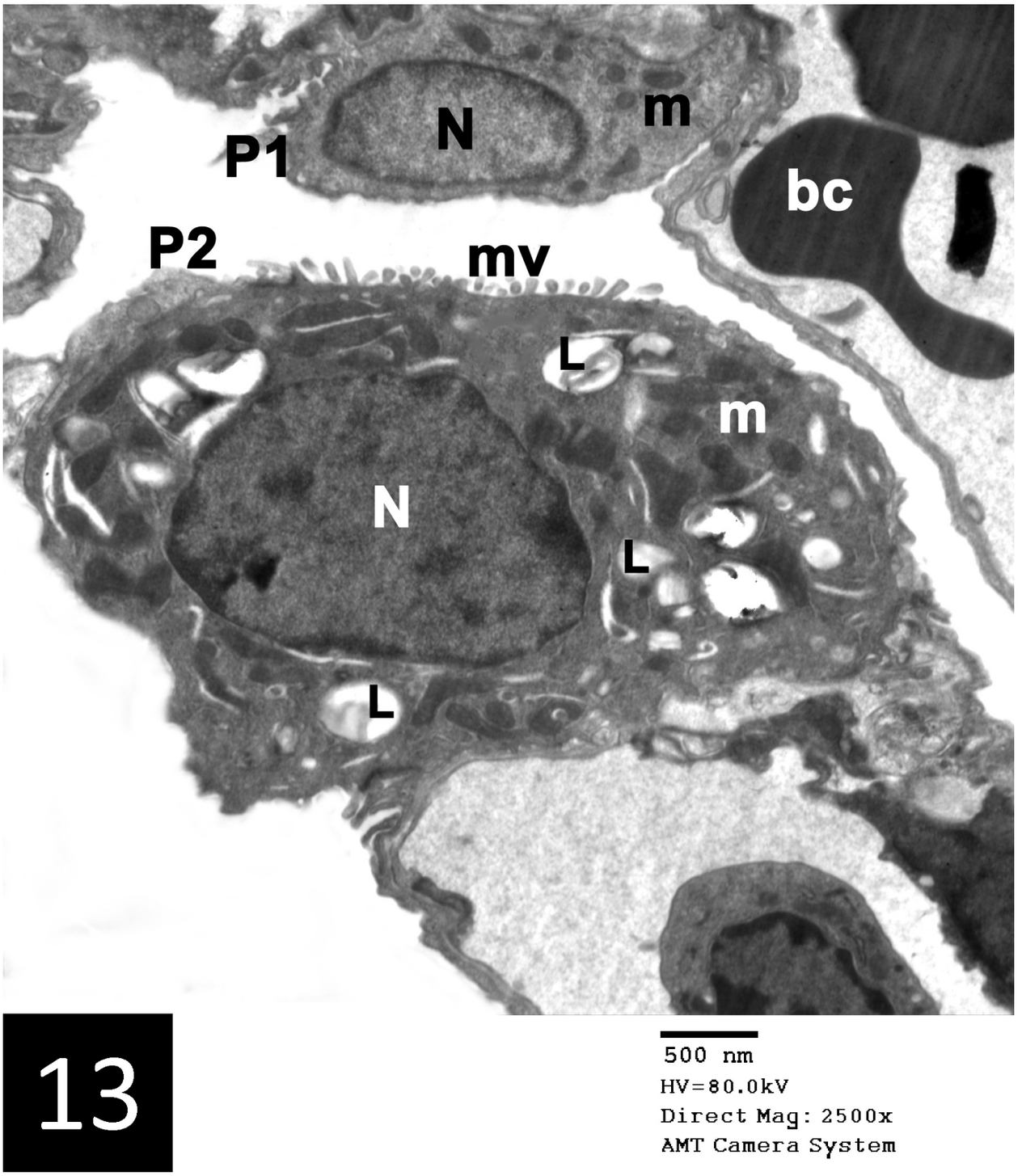

Fig. (13): An electron micrograph of control rat lung showing an alveolus lined by pneumocyte type I (P1) and pneumocyte type II(P2).Type I appears with elongated euchromatic nucleus(N) and mitochondria(m).Pneumocytes type II (P2) shows characteristic microvillous border(mv) and large euchromatic nucleus(N) .Its cytoplasm reveals multiple lamellar bodies(L) and numerous mitochondria(m). Note: interalveolar septum containing blood capillaries (bc). Mic. Mag. x2500

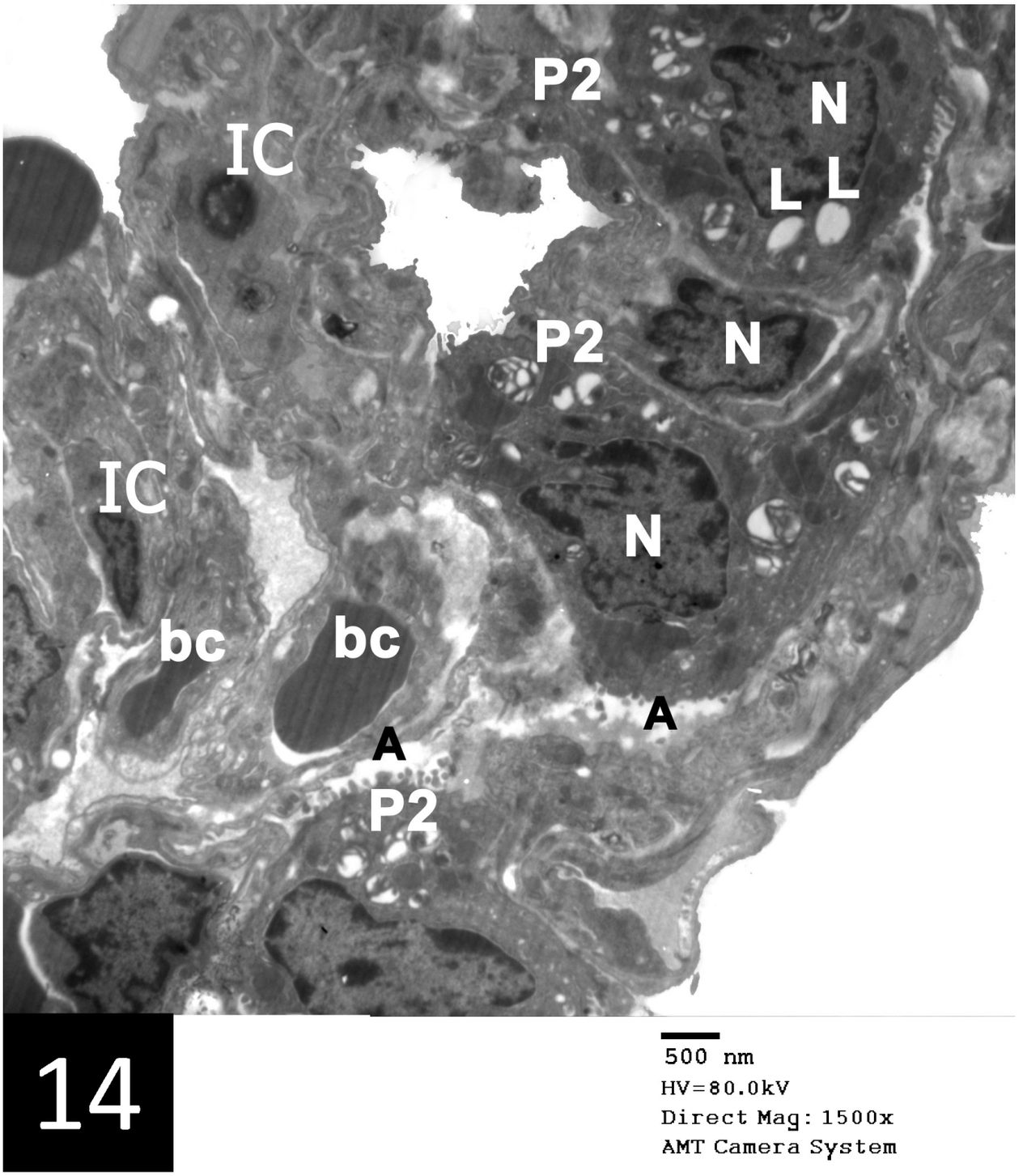

Fig. (14): An electron micrograph of a rat lung subgroup IIA(received pristine MWCNTs, sacrificed after 3 days) showing collapsed alveoli(A)lined mainly with type II pneumocytes (P2) that reveal irregular nuclei(N) with some empty lamellar bodies (L).The interalveoolar septa show interstitial cells (IC) and blood capillaries (bc). Mic. Mag. x1500

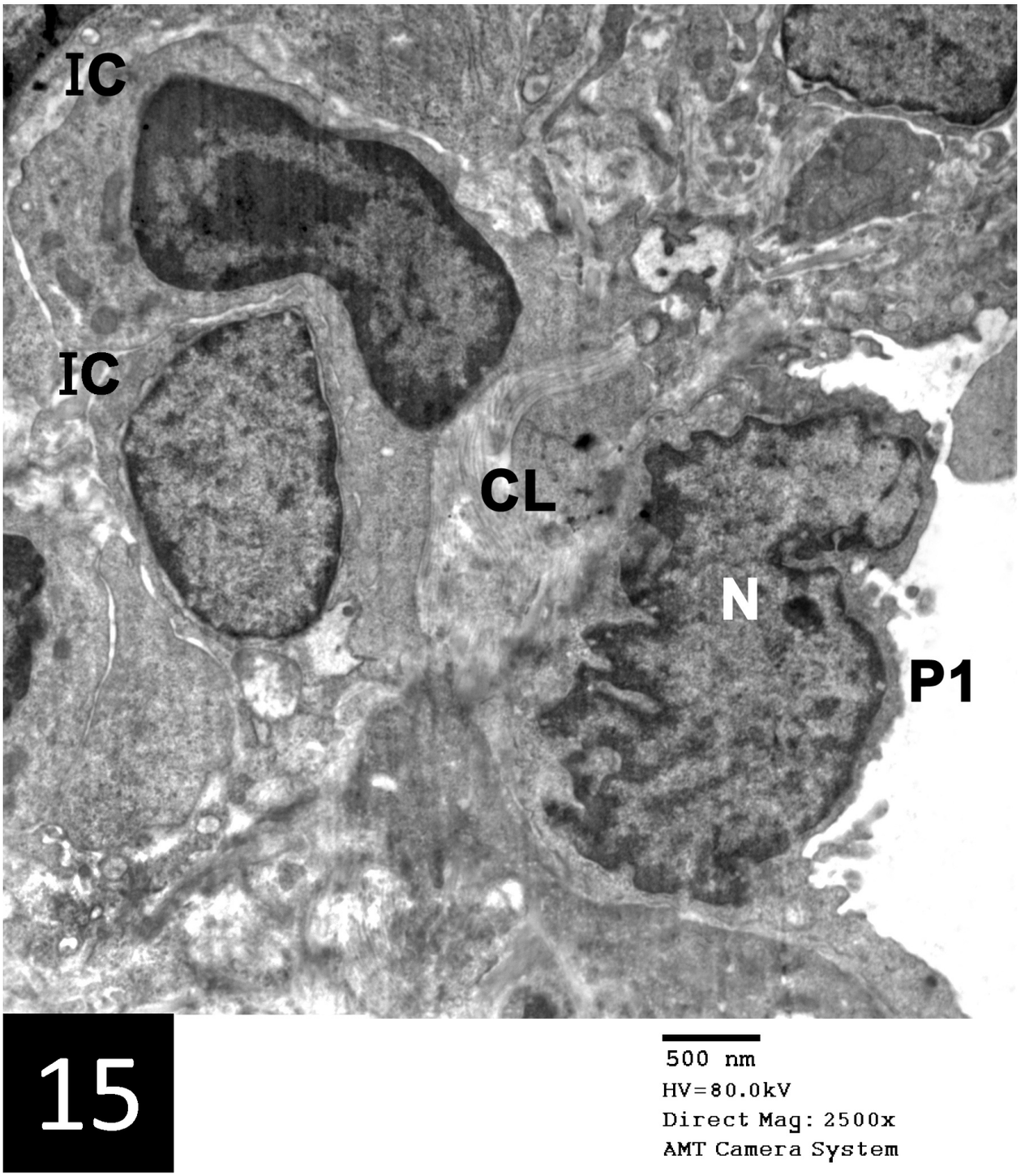

Fig. (15): An electron micrograph of rat lung of subgroup IIA showing an alveolus lined by type I pneumocytes (P1)with irregular nucleus(N).Thick interalveolar septum shows deposition of collagen fibers(CL) and many interstitial cells(IC). Mic. Mag. x 2500

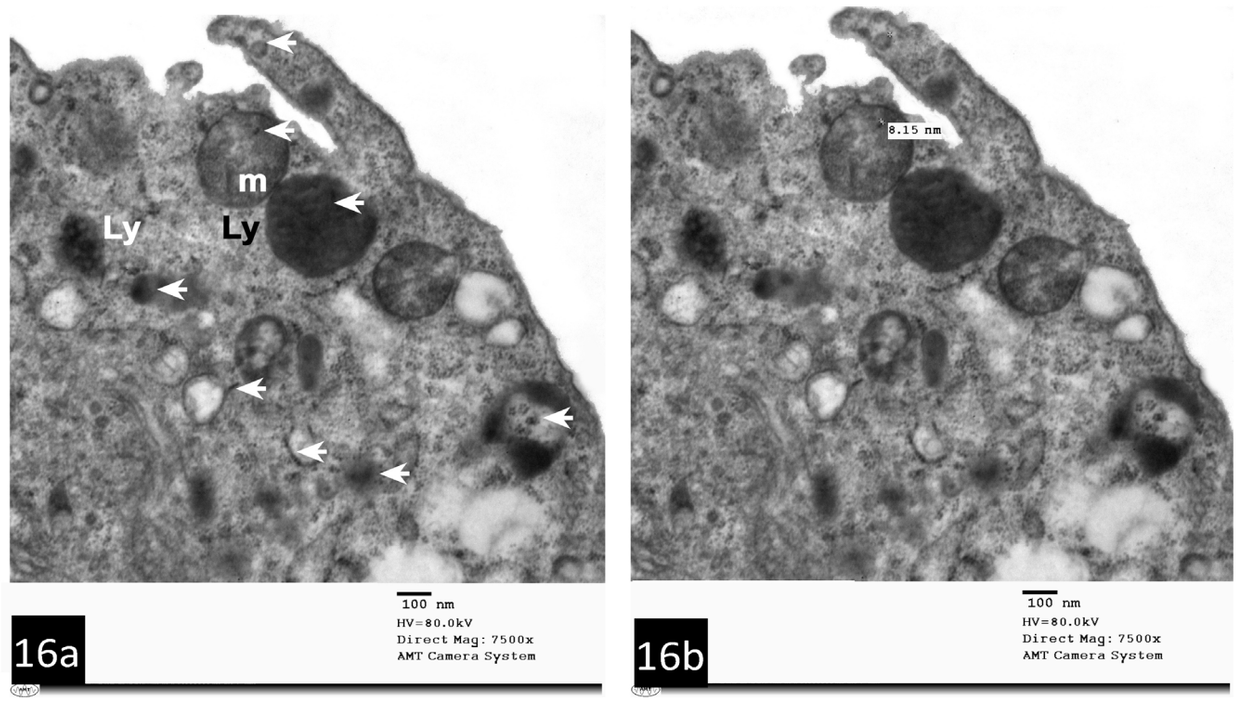

Fig. (16a,b): Electron micrographs of rat lung alveoli group of IIA showing part of alveolar macrophage with cytoplasm rich in electron dense particles(arrow). These particles are also seen inside lysosomes (Ly).Note: mitochondria(m) with distorted cristae and deposits of electron dense nanoparticles(arrow) that measure 8.15nm.Mic.Mag.x 7500

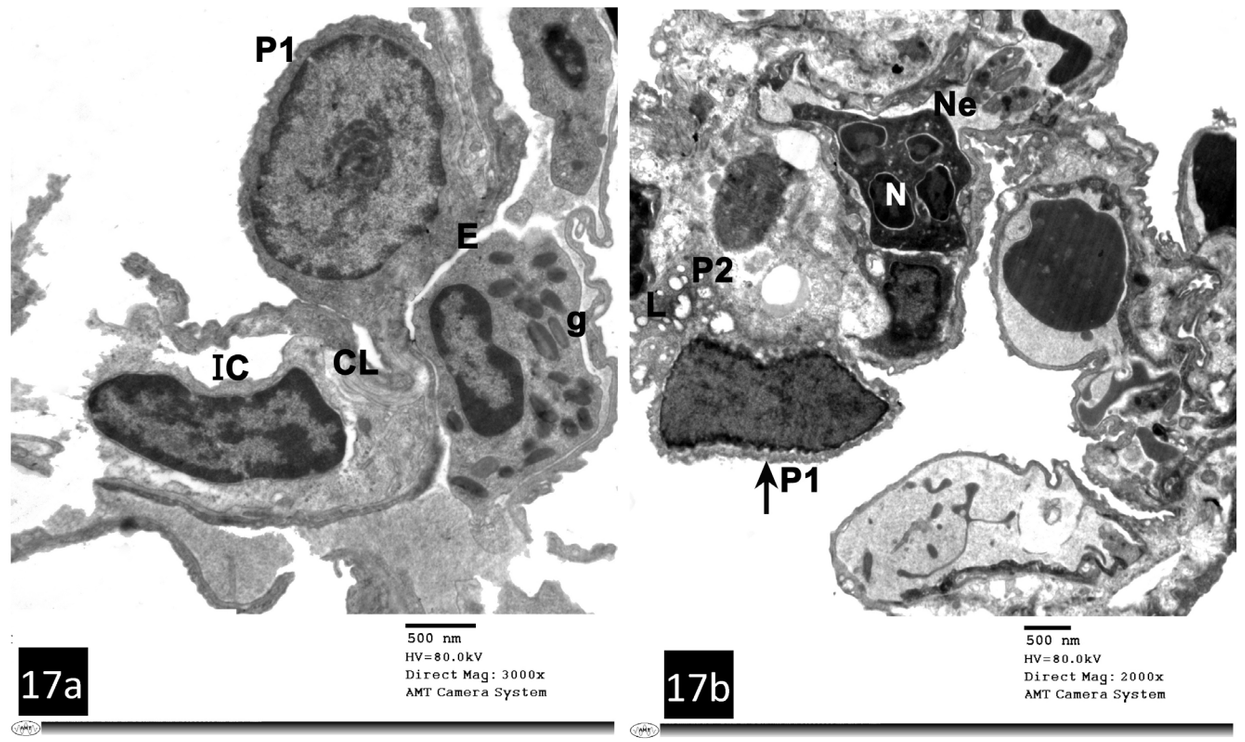

Fig. (17a, b): Electron micrographs of rat lung alveoli of subgroup IIA showing a- Part of an alveolus lined by pneumocyte type I (P1) that bulge into the lumen. Interstitial cell (IC)surrounded by collagen fibers(CL)and eosinophil(E)with its characteristic granules(g) are seen. Mic. Mag. x3000 b- Part of alveolus lined by type II pneumocytes(P2) with empty lamellar bodies(L) and type I pneumocytes(P1) with irregular nucleus bulging into the alveolar cavity. Neutrophil(Ne) with its characteristic segmented nucleus(N)is seen. Mic. Mag. x2000.

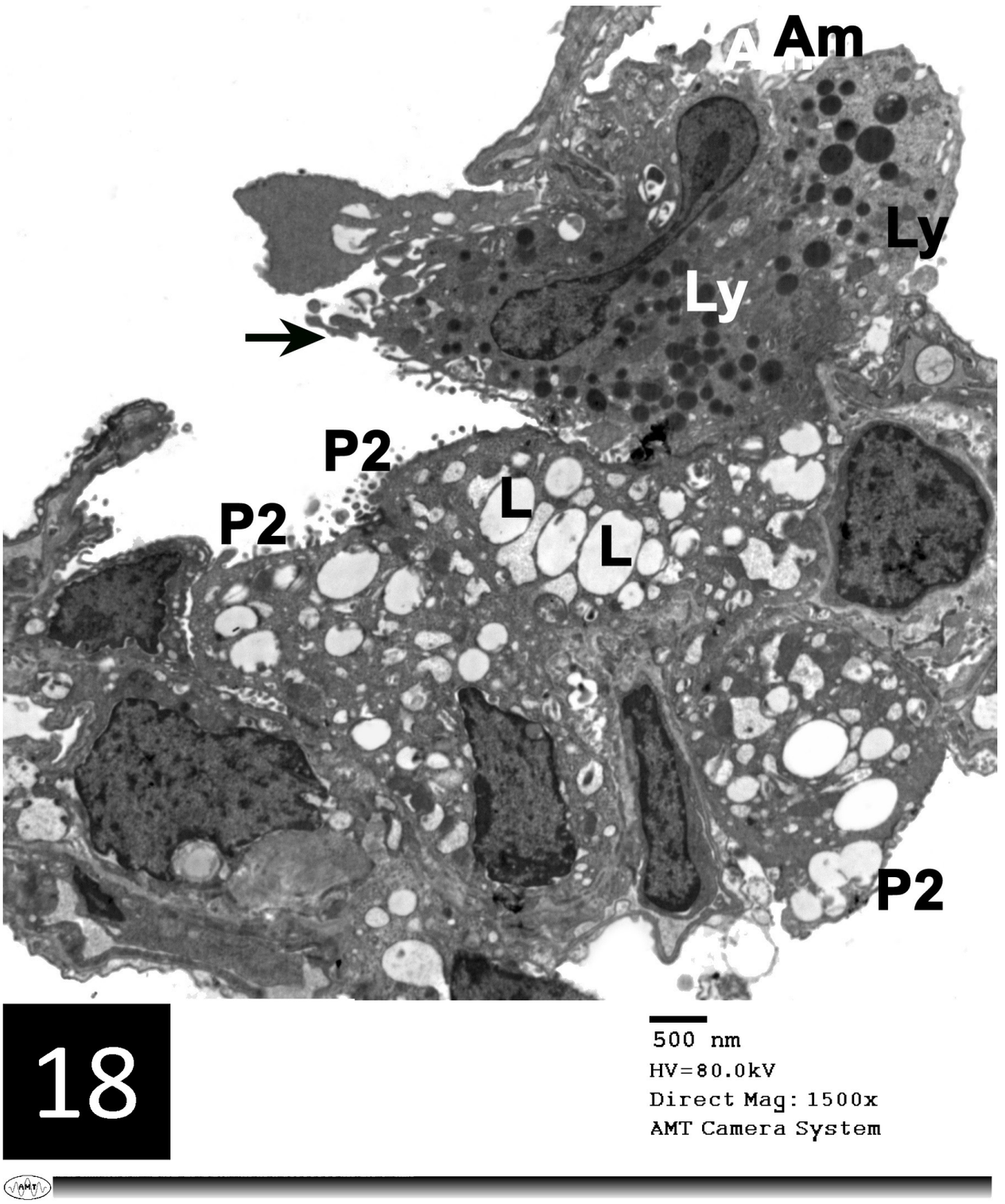

Fig. (18): An electron micrograph of rat lung of subgroup IIB(received pristine MWCNTs, sacrificed after 45 days)showing alveoli lined mainly with type II pneumocytes (P2) that show empty lamellar bodies(L)

Note: Alveolar macrophage (Am)with numerous lamellopodia(arrow) and cytoplasm rich in lysosomes(Ly). Mic. Mag. x 1500

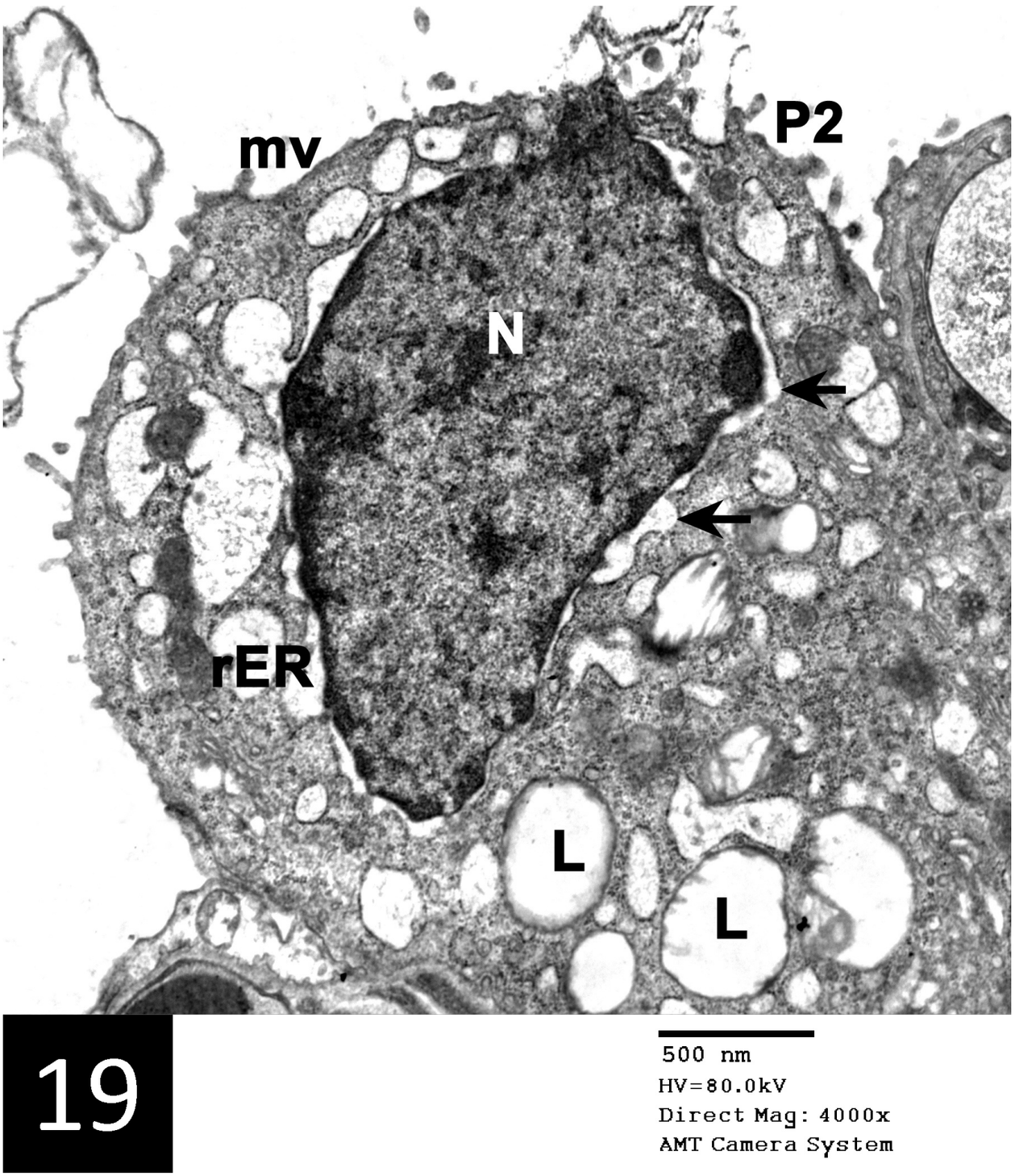

Fig. (19): An electron micrograph of rat lung of subgroup IIB showing an alveolus lined by pneumocytes type II (P2) with blunted microvillous border(mv) and a nucleus(N) with dilated perinuclear cisternae(arrow).The cytoplasm reveals empty lamellar bodies(L) and dilated rough endoplasmic reticulum(rER). Mic. Mag. x 4000

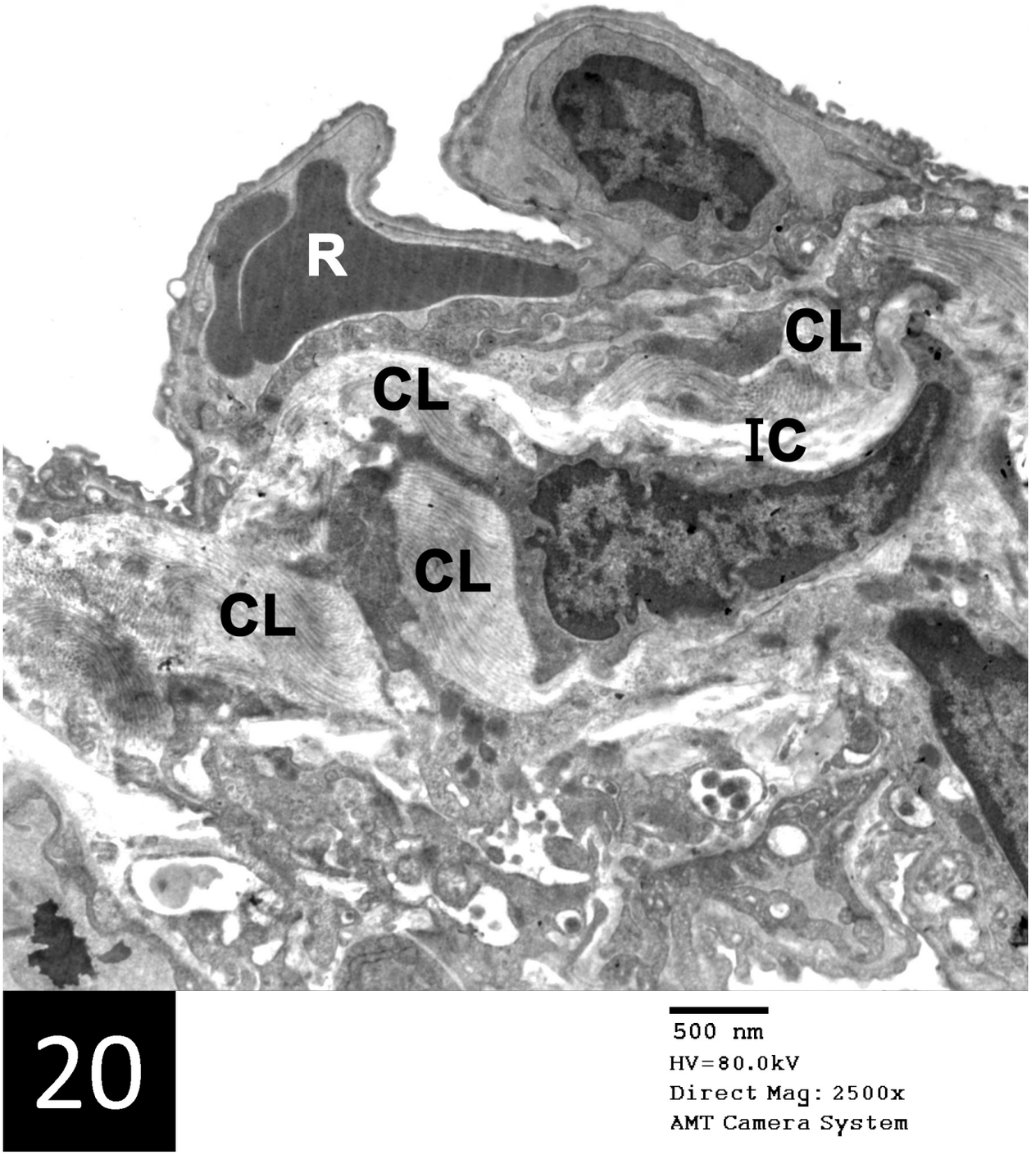

Fig. (20): An electron micrograph of rat lung of subgroup IIB showing thickened interalveolar septum with increased deposition of collagen fibers(CL)around adjacent interstitial cells (IC)Note: blood capillary containing red blood corpuscles (R). Mic. Mag. x 2500

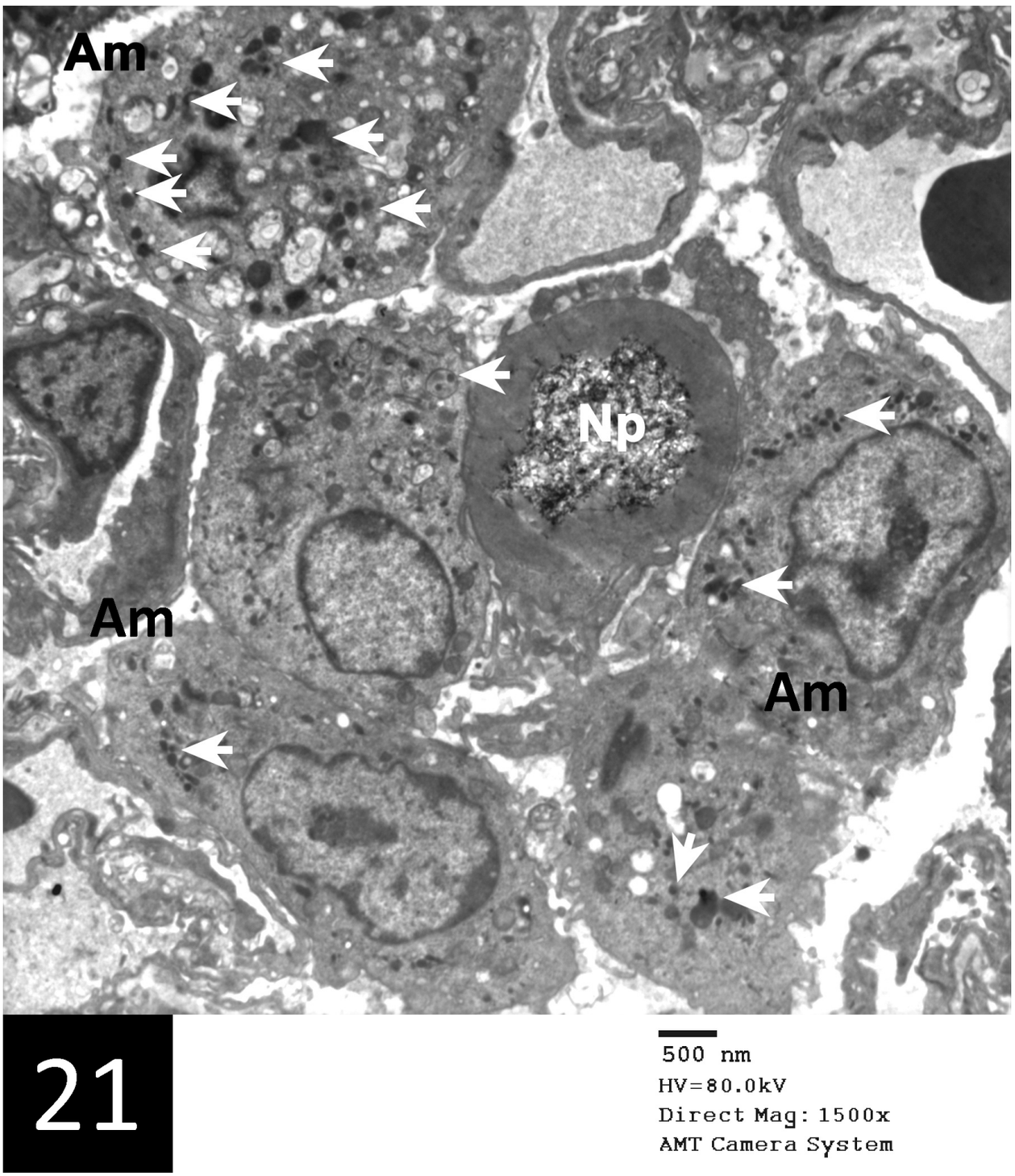

Fig. (21): An electron micrograph of subgroup IIB rat lung showing multiple alveolar macrophages(Am)gathered around a cell containing large aggregates of electron dense nanoparticles (NP). The particles(arrows) are also seen inside the alveolar macrophages either free in the cytoplasm or inside the lysosomes. Mic.Mag.x1500

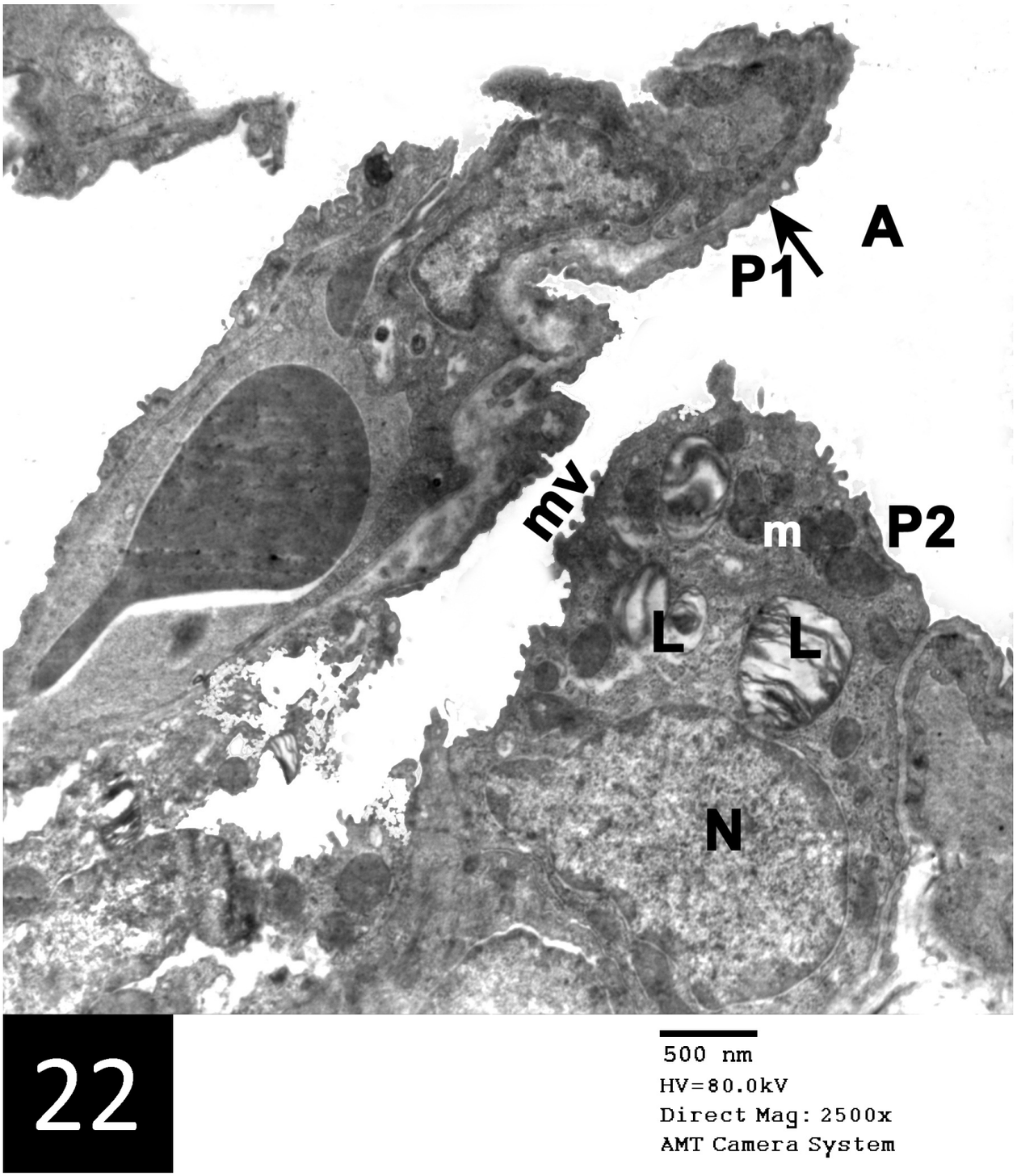

Fig. (22): An electron micrograph of rat lung subgroup IIIA(received PEG-coated MWCNTs ,sacrificed after 3 days) showing thin interalveolar septa and patent alveoli(A),lined by type I pneumocytes (P1 ↑) and type II pneumocytes (P2)with a large vesicular nucleus (N),numerous characteristic lamellar bodies(L)and mitochondria (m). Note: microvillous border of pneumocytes type II(mv). Mic. Mag. x 2500

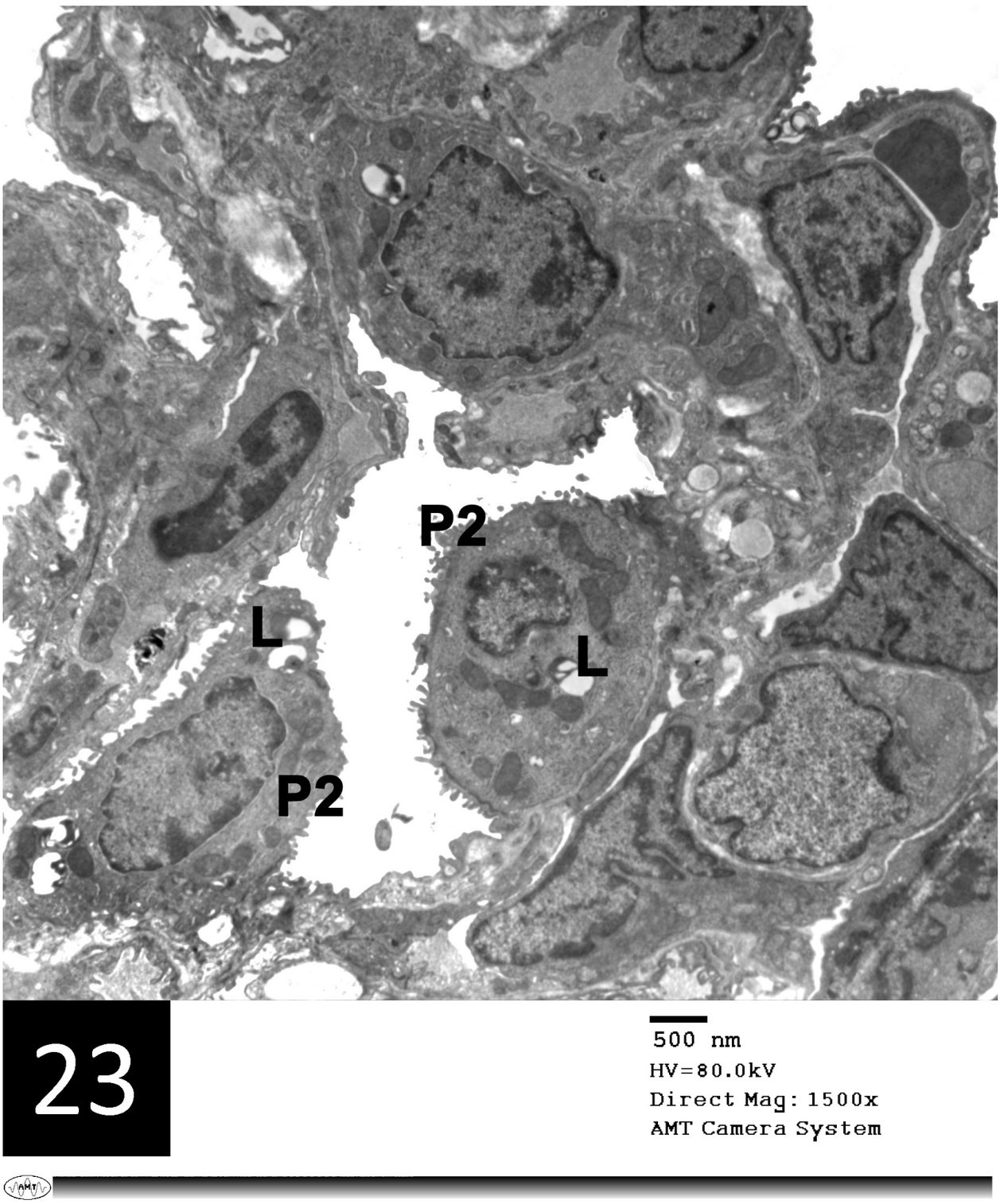

Fig. (23): An electron micrograph of rat lung subgroup IIIA revealing multiple pneumocytes type II (p2)with scanty lamellar bodies(L). Mic Mag. x 1500

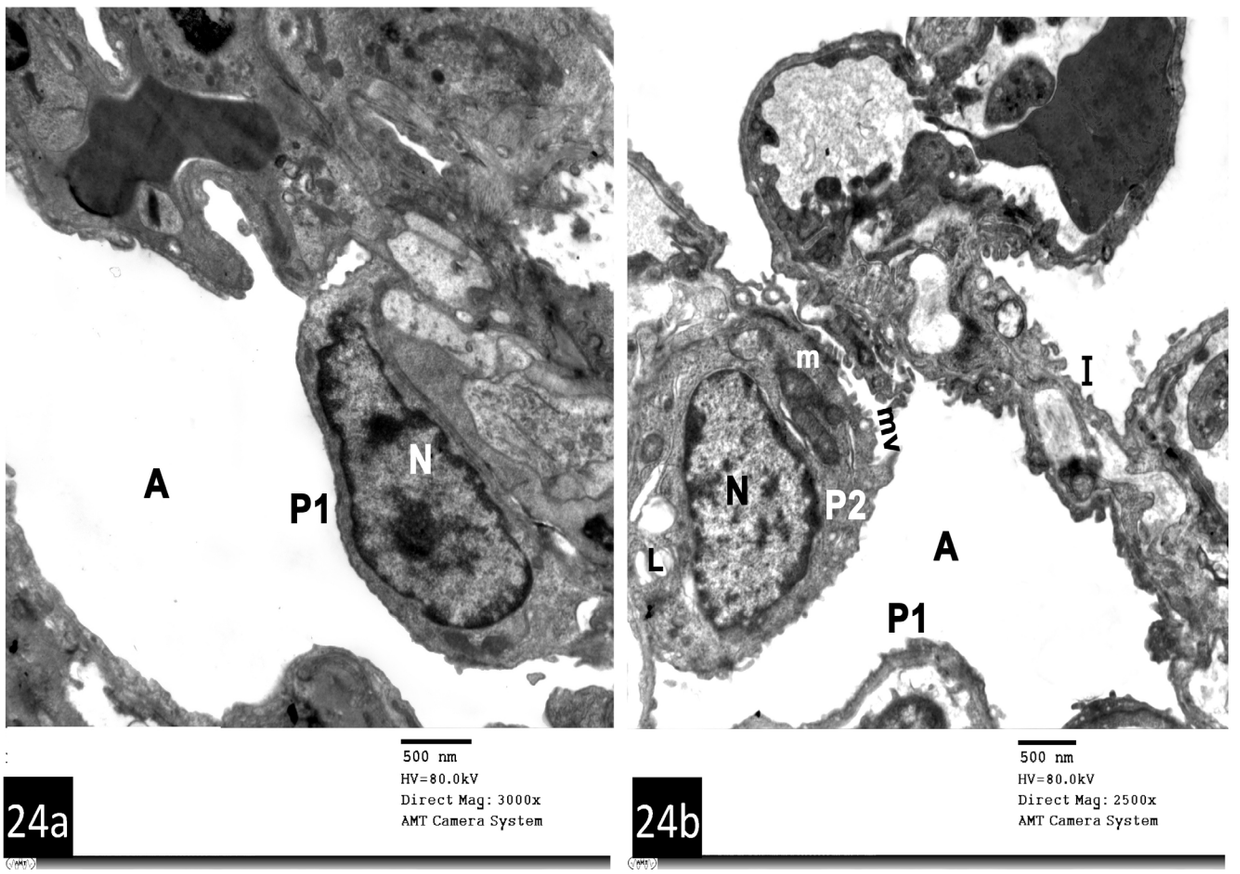

Fig. (24a, b): Electron micrographs of rat lung subgroup of IIIB(received PEG-coated MWCNTs, sacrificed after 45 days)showing a- Type I pneumocyte (P1) with elongated nucleus(N) facing a patent alveolar lumen(A). Mic. Mag. x 3000 b- Well inflated alveolus(A) lined by type I pneumocytes (PI) and type II pneumocyte (P2).Pneumocyte typeII(P2) shows euchromatic nucleus (N) mitochondria(m),lamellar bodies (L)and microvillous border (mv). Note: thin interalveolar septum (I). Mic. Mag x2500

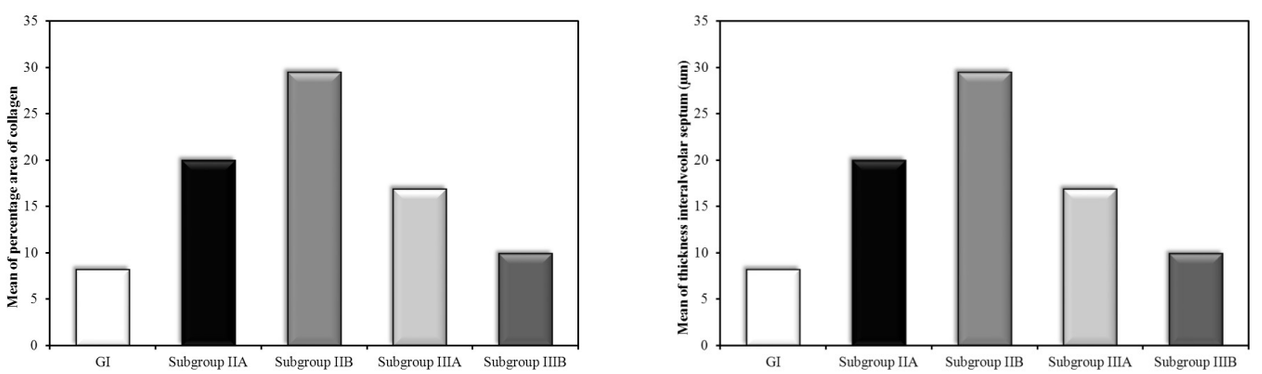

Fig. (25 a, b): a- A bar chart showing comparison between the different studied groups according to percentage area of collagen. b- A bar chart showing comparison between the different studied groups according to thickness of the interalveolar septum.

Table 1: Comparison between the different studied groups according to percentage area of collagen

Percentage area of collagen	Median (Min. – Max.)	Mean ± SD
GI	4.5 (4.5–4.6)	4.5[a]± 0.1
Subgroup IIA	6.5 (5.4–7.5)	6.5[a]±1.5
Subgroup IIB	11.8 (8.9–14.7)	11.8[a]±4.1
Subgroup IIIA	5 (3.3–6.6)	5[a]±2.3
Subgroup IIIB	4.6 (4 –5.2)	4.6[a]± 0.8
F (p)	3.794 (0.088)	

F: F for ANOVA test
p: p value for comparing between the studied groups
Means with Common letters are not significant.

Table 2: Comparison between the different studied groups according to thickness of interalveolar septum (µm)

Thickness of interalveolar septum (µm)	Median (Min. – Max.)	Mean ± SD
GI	6.8 (1.9–21.1)	8.2[b]± 5
Subgroup IIA	18.1 (3.8–87.7)	20[a]±16.9
Subgroup IIB	22.4 (5.1– 142)	29.5[a]±28.5
Subgroup IIIA	15.5 (6.6–33.3)	16.9[a]±8.1
Subgroup IIIB	7.4	9.9[b]±9.8
H (p)	44.505* (<0.001*)	

H: H for Kruskal Wallis test, Pairwise comparison between each 2 groups was done using Post Hoc Test (Dunn's for multiple comparisons test)
p: p value for comparing between the studied groups
*: Statistically significant at $p \leq 0.05$
Means with Common letters are not significant (i.e. Means with Different letters are significant)

DISCUSSION

Exposure to different types of engineered nanomaterials from manufacture to disposal can occur throughout the human life and impacts various harmful effect on the body systems[13] through their ability to cross protective body barriers and accumulate in different organs, so it is important to study not only the torrential applications of NPs but also their adverse effects.[21]

One of the hazardous element of CNTs, which is still under research, is the release of CNTs in aerosol form that is widely inhaled in occupational settings[22]. Experiments in mice have been showed that inhaled CNTs are cleared very slowly from the lungs. It was stated that CNTs have long half-life which is one year[23].

A new era has been developing to minimize CNTs toxicity and accordingly expand their application, in the name of functionalization of CNTs in which new characteristics have been added to them that can't be acquired by ordinary pristine CNTs[13]. Therefore, the present study was planned to investigate the histological effect of pristine MWCNTs and functionalized MWCNTs on lung alveoli of adult albino rat. Tabet *et al*[24] stated that there is a change in the interaction between CNT and the body cell occurring by time, which necessitate the study of such interaction at various time points. Therefore, in the present study two different time points (3and 45 days) were chosen.

In the current study, the intratracheal administration was chosen as a method of administration. Even though, in human exposure, inhalation is considered as the natural route of entry, this method cannot always be used for various reasons including large quantity of test substances that are needed and the high price of the inhalation equipment. Moreover, the intratracheal instillation delivered the actual dose to the lung, which can be accurately measured. Therefore, intratracheal instillation has been engaged in several researches as an alternative exposure route[25-27].

The present study clearly indicated that pristine MWCNTs administration resulted in various histological changes in the lung architecture. These changes were more obviously after 45 days. Collapsing of the alveoli that was observed in the present study were reported by many authors[28,29] which could be explained by either failure of the alveoli to expand as a result of inflammation[29] or surfactant dysfunction as a consequence of deformity in the shape and decrease in the number of the lamellar bodies[28] On the other hand, overexpansion of some alveoli that was also noticed in this study could be explained by the progressive degradation of pulmonary elastin that resulted from exposure to relevant doses of carbon nanoparticles[30].

Morphometrical and statistical analysis performed in the current work confirmed the histological result. They showed significant increased thickening of interalveolar septa in subgroup IIA and IIB that received pristine MWCNTs as compared to the control group.This finding could be attributed to marked cellular infiltration especially noticed in the perivascular and peribronchiolar areas with increase collagen deposition.The present results were inaccordance with Krestina *et al* and Mitchell *et al*[27,31] who stated that after inhalation of MWCNTs, an increase in inflammatory cells have been observed. Moreover, Boyles *et al*[32] reported that rapid recruitment of neutrophils, eosinophils and even macrophages occurred after inhalational exposure to carbon nanotubes.

Proliferation of type II pneumocytes were frequently encountered in the present study. It was attributed to damage of type I pneumocytes as they are quite sensitive to toxins. Thus, type II pneumocytes start a burst of division to replace the damaged cells and restore the integrity of the alveolar epithelium. Proliferation was found to start taking place approximately 2 to 3 days following intratracheal instillation of toxins[33].

The deposition of collagen fibers seen in examined lung tissue in rats in group II especially after 45 days of administration of pristine MWCNTs was analyzed morphometrical and statitical. The result showed that there was increase in the percentage area of collagen in this group as compared to the control group although it was still statistically insignificant which could be explained by shorter duration that needed to establish chronic lung fibrosis. However, the role of CNTs in induction of rapid onset inflammatory and fibrotic changes which preceeded chronic pulmonary fibrosis, could not be excluded[34].

The noticed collagen deposition was in accordance with many researchers[27,35,36]. They revealed that lung fibrosis might result from the liberation of mediators such as cytokines and oxidants from accumulated leukocytes. Moreover, Vietti *el al*[37] noticed activation of resident fibroblasts or bone marrow progenitor cells as a result of chronic inflammation with subsequent proliferation and differentiation of these cells into myofibroblasts. Furthermore, He X *et al*[38] reported that the alveolar epithelial cells can be transformed into myofibroblasts, a process known as epithelial mesenchymal transition.

Recent study done by Jie D *et al*[39] highlighted another key factor in induction of lung fibrosis which is activation of a subset of lung macrophages that promote the development of fibrosis by provoking an environment rich in pro-fibrotic cytokines and growth factors with subsequent activation of fibroblasts and even myofibroblasts lead to production of an excess extracellular matrix.

A constant feature of the examined lung tissue that recieved MWCNTs is the prescence of dark deposits distributed in the interstitium,alveolar spaces as well as inside alveolar macrophages.Similar finding was reported by many researchers[26.27,30,40] who reported the observation of MWCNTs on the light and electron microscopic levels in the lungs following their phagocytosis by alveolar macrophages and consecutively accumulated in the alveoli. In accordance with Kristina *et al*[27] and Mercer *et al*[41], the bulk of MWCNTs lung was found in the alveolar macrophages, while small percentage was found within the alveolar interstitium.

It has been clarified that the cytoplasm and nuclear changes observed in pneumocytes and interstitial cells in this study suggest that nanoparticles interfere with antioxidant defense mechanisms with subsequent generation of excess reactive oxygen species (ROS)[42]. Accordingly, the exact mechanism by which CNTs can cause their toxic effect on lung tissues is oxidative stress where there is disruption of balance between antioxidant power of target cells and ROS. These ROS interact with critical cellular macromolecules leads to their oxidative damage[43].

In the present study, animals received PEG-coated MWCNTs revealed considerable preservation of the alveolar architecture which was confirmed by morphometrical and statistical analysis. These findings suggested that functionalized PEG-coated MWCNTs resulted in considerable improving effect on the lung tissue.

Undoubtedly, Lacerda *et al*[44] stated that PEG possesses its biocompatibility and good solubility under various physiological conditions. In the context of this study, Yang *et al*[43] recommended that reduction of the cytotoxicity of pristine SWCNTs occurred via functionalization. Meanwhile, Liu *et al*[16] stated that surface functionalization chemistry is the most fundamental factor in minimizing CNT toxicity. PEG –coating on CNTs, convey an inertness in biological environments, thus, reducing the toxicity of CNTs.

So far, Tabet *et al*[24] stated that functionalized polymers suppressed the cytotoxicity, oxidative stress and inflammation induced by pristine MWCNTs by reduction in the amount of the nanotube materials supplied by uncoated pristine together with prevention of adherence of coated MWCNTs to the cell membrane with subsequent decrease in its internalization and penetration inside the cell. Moreover, the coated MWCNTs possess abundance of ozone oxidizable groups on their surface, so once they internalized inside the cell, they may act as free radical scavengers, in that way reducing the oxidative stress and the following inflammation[24, 45].

Moreover, Yang *et al*[46] reported that the functionalization of MWCNTs can reduce their rate of accumulation in body tissues. They concluded that comparatively, functionalized MWCNTs have a lesser degree of accumulation than pristine, most likely due to the high individualization of functionalized-MWCNTs.

Taken together, the present study reinforces the concept that pristine MWCNTs greatly affect the lung tissues of the adult male albino rats. Nevertheless, these changes could be ameliorated by PEG functionalization.

CONFLICT OF INTEREST

There are no conflict of interest.

REFERENCES

1. Sa Sandra, Yasuhito S, Sahoko I, Masayuki K, Wenting W, Toshio T, *et al*. Toxicological Evaluation of SiO2 Nanoparticles by Zebrafish Embryo Toxicity Test. Int J Mol Sci 2019;20(1) :882-900.
2. Magdalena R, Agnieszka J, Karolina S, Iza K, Mirosława K, Elżbieta A, et al. The toxicity in *vitro* of titanium dioxide nanoparticles modified with noble metals on mammalian cells. Int J Appl Ceram Technol 2019;16(2):481–93.
3. Arman J, Shadi H, Mohammad B, Amir E, Farnaz G, Negar A. Effect of organic/inorganic nanoparticles on performance of polyurethane nanocomposites for potential wound dressing applications. Journal of the Mechanical Behavior of Biomedical Materials 2018;88 (2): 395-405.
4. López-Serrano A, Olivas RM,Landaluzea JS, Cámara C. Nanoparticles: a global vision. Characterization, separation, and quantification methods. Potential environmental and health impact. Anal Methods 2014;6(5): 38-56.
5. Manfredi A, Dimitrios K, Massimiliano G, Martina C, Alessandra P, Malamatenia A, *et al*. Toxicity determinants of multi-walled carbon nanotubes: The relationship between functionalization and agglomeration. Toxicology Reports 3,2016(2): 230–43.

6. Min-H, Yu S. Effects of functionalized multi-walled carbon nanotubes on toxicity and bioaccumulation of lead in Daphnia magna. PLOS ONE 2018; 13(3): 432-44.
7. Pereira MM, M outon L, Yéprémian C, Couté A, Lo J, Marconcini JM, *et al*. Ecotoxicological effects of carbon nanotubes and cellulose nanofibers in Chlorella vulgaris. J Nanobiotechnology 2014; 22(4): 12-15.
8. Eşref Demir, Ricard Marcos. Toxic and genotoxic effects of graphene and multi-walled carbon nanotubes. Journal of Toxicology and Environmental Health, Part A 2018; 81(14):645-60.
9. Zhang X, Meng L, Lu Q, Fei Z, Dyson PJ. Targeted delivery and controlled release of doxorubicin to cancer cells using modified single wall carbon nanotubes. Biomaterials 2009; 30(30):6041–7.
10. Pedro M, Viviana N, Adrian E, José Luis M, Paloma B, Monica M. Effects at molecular level of multi-walled carbon nanotubes (MWCNT) in Chironomus riparius (DIPTERA) aquatic larvae. Aquat Toxicol 2019; 209(1) : 42-8.
11. De Matteis V. Exposure to Inorganic Nanoparticles: Routes of Entry, Immune Response, Biodistribution and In *Vitro*/In *Vivo* Toxicity Evaluation.Toxics 2017 ; 5(4): 29-33.
12. Kam NWS, Liu Z, Dai H. Functionalization of Carbon Nanotubes via Cleavable Disulfide Bonds for Efficient Intracellular Delivery of siRNA and Potent Gene Silencing. J Am Chem Soc 2005; 127(36): 12492-3.
13. Coccini T, Manzo L, Roda E. Safety evaluation of engineered nanomaterials for health risk assessment: an experimental tiered testing approach using pristine and functionalized carbon nanotubes. ISRN Toxicol 2013; 2013(5):1-13.
14. Saito N, Haniu H, Usui Y, Aoki K, Hara K, Takanashi S, *et al*. Safe clinical use of carbon nanotubes as innovative biomaterials. Chem Rev 2014; 114(11):6040-79.
15. T.P. Dyachkova, A.V. Rukhov, A.G. Tkachev, E.N. Tugolukov. Functionalization of Carbon Nanotubes: Methods, Mechanisms and Technological Realization. Advanced Materials and Technologies 2018; 2 (1): 18-41.
16. Liu Z, Tabakman SM, Chen Z, Dai H. Preparation of carbon nanotube bioconjugates for biomedical applications. Nat Protoc 2009;4(9):1372-82
17. Warheit DB. How meaningful are the results of nanotoxicity studies in the absence of adequate material characterization? Toxicol Sci 2008;101(2):183-5.
18. Osswald S, Havel M, Gogotsi Y. Monitoring oxidation of multiwalled carbon nanotubes by Raman spectroscopy. J Raman Spectrosc2007;38(6):728–36.
19. Carleton HM, Drury RAB, Wallington EA. Carleton's Histological Technique. 5th ed. Oxford, New York, Toronto: Oxford University Press; 1980. 140-2.
20. Bancroft JD, Gamble M. Theory and practice of histological techniques. 6th ed. Philadelphia: Churchill Livingstone Elsevier; 2008. 601-41.
21. Valentini X, Rugira P, Frau A, Tagliatti V, Conotte R, Laurent S,*et al*. Hepatic and renal toxicity induced by TiO2 nanoparticles in rats: A morphological and metabonomic study. J Toxicol 2019;223(3):331-350.
22. Reddy AR, Reddy YN, Krishna DR, Himabindu V. Pulmonary toxicity assessment of multiwalled carbon nanotubes in rats following intratracheal instillation. Environ Toxicol 2012;27(4):211-9.
23. Køobler C, Poulsen SS, Saber AT, Jacobsen NR, Wallin H, Yauk CL, *et al*. Time-dependent subcellular distribution and effects of carbon nanotubes in lungs of mice.PLoS One 2015;10(1):415-26.
24. Tabet L, Bussy C, Setyan A, Simon-Deckers A, Rossi MJ, Boczkowski J, *et al*. Coating carbon nanotubes with a polystyrene-based polymer protects against pulmonary toxicity.Part FibreToxicol 2011;8(3):1-13
25. Zhu MT, Feng WY, Wang Y, Wang B, Wang M, Ouyang H, *et al*. Particokinetics and extrapulmonary translocation of intratracheally instilled ferric oxide nanoparticles in rats and the potential health risk assessment. Toxicol Sci 2009; 107(2): 342-51.
26. Kobayashi N, Naya M, Ema M, Endoh S, Maru J, Mizuno K, *et al*. Biological response and morphological assessment of individually dispersed multi-wall carbon nanotubes in the lung after intratracheal instillation in rats. Toxicology 2010; 276(3):143-53.
27. Kristina B, Trine B, Petra J, Sarah S, Alicja M, Nicklas R, *et al*. Nanotube induced pulmonary histopathology and toxicity one year after pulmonary deposition of 11 different Multiwalled carbon nanotubes in mice. Basic Clin Pharmacol Toxicol 2019;124(5):211–27.
28. Schleh C, Mühlfeld C, Pulskamp K, Schmiedl A, Nassimi M, Lauenstein H, *et al*. The effect of titanium dioxide nanoparticles on pulmonary surfactant function and ultrastructure. Respir Res 2009; 10(1): 90-101.

29. Wang X, Katwa P, Podila R, Chen P, Ke PC, Rao AM, *et al*. Multi-walled carbon nanotube instillation impairs pulmonary function in C57BL/6 mice. Part Fibre Toxicol 2011;8(3):8-24.

30. Agnès R, Lucie A, Maylis D, Françoise R, Angélique S, Esther B, *et al*. Intratracheally administered titanium dioxide or carbon black nanoparticles do not aggravate elastase-induced pulmonary emphysema in rats. BMC Pulmonary Medicine 2012;12(2) :38-50.

31. Mitchell LA, Gao J, Wal RV, Gigliotti A, Burchiel SW, McDonald JD. Pulmonary and systemic immune response to inhaled multiwalled carbon nanotubes. Toxicol Sci 2007; 100(1):203-14.

32. Boyles MS, Stoehr LC, Schlinkert P, Himly M,Duschl A. The significance and insignificance of carbon nanotube-induced inflammation. Fibers 2014; 2(5): 45-74.

33. Honda T, Ota H, Yamazaki Y, Yoshizawa A, Fujimoto K, Sone S. Proliferation of type II pneumocytes in the lung biopsy specimens reflecting alveolar damage. Respir Med. 2003;97(1):80-5.

34. Dong J and Ma Q. In *vivo* activation of a T helper 2-driven innate immune response in lung fibrosis induced by multi-walled carbon nanotubes. Archives of Toxicology2016; 90(10):2231–48.

35. Muller J, Huaux F, Moreau N, Misson P, Heilier JF, Delos M, *et al*. Respiratory toxicity of multi-wall carbon nanotubes. Toxicol Appl Pharmacol 2005;207(3):221–31.

36. Lee BW,Kadoya C, Horie M, Mizuguchi Y, Hashiba M, Kambara T, *et al*. Analysis of pulmonary surfactant in rat lungs after intratracheal instillation of short and long multi-walled carbon nanotubes. Inhal Toxicol 2013; 25(11): 609–20.

37. Vietti G, Lison D, van den Brule S. Mechanisms of lung fibrosis induced by carbon nanotubes: towards an Adverse Outcome Pathway (AOP).Part Fibre Toxicol 2016; 13(12):11-34.

38. He X, Young SH, Schwegler-Berry D, Chisholm WP, Fernback JE, Ma Q. "Multiwalled carbon nanotubes induce a fibrogenic response by stimulating reactive oxygen species production, activating NF-$_k$B signaling, and promoting fibroblast to-myofibroblast transformation. Chemical Research in Toxicology 2011; 24 (12): 2237–48.

39. Jie D and Qiang M. Macrophage polarization and activation at the interface of multiwalled carbon nanotube-induced pulmonary inflammation and fibrosis. Nanotoxicology 2018 ; 12(2): 153–68.

40. Elgrabli D, Floriani M, Abella-Gallart S, Meunier L, Gamez C, Delalain P, *et al*. Biodistribution and clearance of instilled carbon nanotubes in rat lung. Part Fibre Toxicol 2008; 5(4):20-33.

41. Mercer RR, Hubbs AF, Scabilloni JF, Wang L, Battelli LA, Friend S, *et al*. Pulmonary fibrotic response to aspiration of multi-walled carbon nanotubes. Part Fibre Toxicol 2011; 8(5):21-32.

42. Alarifi S, Ali D, Alkahtani S, Alhader MS. Iron oxide nanoparticles induce oxidative stress, DNA damage, and caspase activation in the human breast cancer cell line. Biol Trace Elem Res 2014; 159(3):416-24.

43. Yang ST, Wang X, Jia G, Gu Y, Wang T, Nie H, *et al*. Long-term accumulation and low toxicity of single-walled carbon nanotubes in intravenously exposed mice. Toxicol Lett 2008; 181(3):182-9.

44. Lacerda L, Ali-Boucetta H, Herrero MA, Pastorin G, Bianco A, Prato M, *et al*. Tissue histology and physiology following intravenous administration of different types of functionalized multiwalled carbon nanotubes. Nanomedicine (Lond) 2008; 3(5):149–61.

45. Miao Y, Shaohui H, Kevin J, Alisa M. Dextran and polymer polyethylene glycol (PEG) coating reduce both 5 and 30 nm iron oxide nanoparticle cytotoxicity in 2D and 3D cell culture. Int J Mol Sci 2012; 13 (3): 5554-70.

46. Yang ST, Luo J, Zhou Q, Wang H. Pharmacokinetics, metabolism and toxicity of carbon nanotubes for biomedical purposes. Theranostics 2012; 2(3): 271-82.

الملخص العربى

دراسة هستولوجية لتأثيرالانابيب الكربونية المتناهية الصغر و المتعددة الجدران الاصلية مقابل الموظفة بمجموعة البولى ايثيلين جليكول على الحويصلات الهوائية فى ذكورالجرذان البيضاء البالغة

صافيناز حسين صفوت، إيمان نبيل، وحيد مفيد اسطفانوس، ومروة مجدي

كلية الطب ـ جامعة الإسكندرية ـ الإسكندرية

المقدمة: تستخدم الأنابيب الكربونية المتناهية الصغر تجارياً فى مختلف التطبيقات ولكن سميتها على أنسجة الجسم المختلفة جعل لها تأثير فعال على صحة الإنسان، لذلك فإن توظيفها ظهر كأداة لتقليل سمية هذه الأنابيب وبالتالى توسيع تطبيقاتها بدون تهديد لحياة الإنسان.

الهدف من البحث: تهدف هذه الدراسة لتسليط الضوء على تأثير الأنابيب الكربونية الأصلية المتناهية الصغر ومتعددة الجدران على الحويصلات الهوائية للرئة فى ذكور الجرذان البيضاء البالغة وإمكانية إضعاف هذا التأثير عن طريق توظيفها بمجموعة البولى ايثيلين جليكول.

مواد وطرق البحث: أجريت هذه الدراسة على ٦٠ من ذكور الجرذان البيضاء البالغة (١٥٠ – ٢٠٠جم)، تم تقسيمهم الى ثلاث مجموعات:

• المجموعة الأولى: وشملت ٢٠ فأر تم تقسيمهم إلى مجموعتين فرعيتين أشتملت كل مجموعة على ١٠ فئران وتم اعطائها ١ مل/كجم من وزن الجسم محلول ملح داخل القصبة الهوائية مرة واحدة فى بداية التجربة وتم ذبحها بعد ٣ أيام للمجموعة الفرعية الأولى، و٤٥ يوم للمجموعة الفرعية الثانية.

• المجموعة الثانية: تم تقسيمها إلى مجموعتين فرعيتين اشتملت كل مجموعة على ١٠ فئران وتم اعطائها ١ مج/كجم من وزن الجسم من الأنابيب الكربونية الأصلية المتناهية الصغر والمتعددة الجدران داخل القصبة الهوائية مرة واحدة فى بداية التجربة وتم ذبحها بعد ٣ أيام للمجموعة الفرعية الأولى، و٤٥ يوم للمجموعة الفرعية الثانية.

• المجموعة الثالثة: تم تقسيمها مثل المجموعة الثانية وتم اعطائها ١ مج/كجم من وزن الجسم من الأنابيب الكربونية المتناهية الصغر والمتعددة الجدران والموظفة بمجموعة البولى ايثيلين جليكول داخل القصبة الهوائية مرة واحدة فى بداية التجربة وتم ذبحها مثل المجموعتين السابقتين.

فى نهاية التجربة، أخذت عينات الرئة وتم تحضيرها للفحص بالمجهر الضوئى والإلكترونى، وتم قياس سمك الحاجز ما بين الحويصلات الهوائية وقياس مساحة الكولاجين وتحليلها إحصائياً.

النتائج:أظهر الفحص بأن أنابيب الكربون الأصلية المتناهية الصغر والمتعددة الطبقات تسببت فى تغيرات نسيجية بدرجات متفاوتة على رئة الحيوانات وكانت هذه التغيرات أكثر وضوحاً بعد ٤٥ يوم وظهرت على هيئة حويصلات

هوائية ضيقة وأخرى واسعة، ازدياد سمك الحواجز بين الحويصلات، ازدياد ترسب الكولاجين،احتقان فى الاوعية الدموية مع انصباب دمى لكرات الدم الحمراء. كما ظهرت تغيرات فى الخلايا والنوات مع تراكم الخلايا الآكلة والمحملة بجزيئات الكربون بداخل الحويصلات الهوائية والحواجز التى بينها. كما اظهر الفحص بالمجهر الالكترونى عن حدوث تغيرات تحللية للخلية الرئوية من النوع الثاني و ازدياد عددها .هذه التغيرات ظهرت أقل وضوحاً بكثير فى المجموعة المستقبلة للأنابيب الكربونية المتناهية الصغر والمتعددة الجدران والموظفة بالبولى ايثلين جليكول مع الإحتفاظ الى درجة ما بالتركيب الطبيعى للحويصلات الهوائية.

الاستنتاج: أوضحت هذه الدراسة أن الأنابيب الكربونية الأصلية المتناهية الصغر والمتعددة الجدران لها تأثير سام على النسيج الرئوى، وهذا التأثير يمكن تقليله بتوظيف الأنابيب الكربونية المتناهية الصغر بمجموعة البولى ايثلين جليكول.